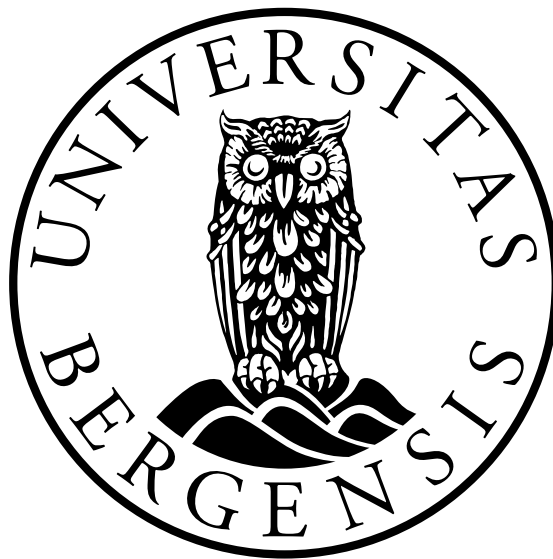


# **Factors influencing interannual variability of Belg rain in Ethiopia**

**Carina Knudsen**



Supervisors: Lea Svendsen, Noel Keenlyside  
Erik Kolstad

01/03/23



# Acknowledgements

I want to thank my supervisors for their advice, continuous feedback, and support. You have made this journey enjoyable and manageable. I especially would like to thank my main supervisor Lea Svendsen for our weekly meetings bringing motivation and feedback. I would also like to thank Tarkan Aslan Bilge for helping access the model data and Teferi Dejene Demissie for many helpful advice and a nice meeting in the start phase of this thesis. Further, I would like to thank my partner, family, and fellow students at GFI for always being there for me and showing continuous support. I would also like to thank Christine Calvert for giving feedback on my writing.

NOAA Optimum Interpolation (OI) SST V2 data used in this thesis was provided by the NOAA PSL, Boulder, Colorado, USA, from their website (<https://psl.noaa.gov>). ECMWF provided the ERA5 data. Acknowledge is also given to Michael Sprenger (ETH Zurich) for the support in providing the data. The CHIRPS monthly and daily products are provided by the Climate Hazards Center (CHC), UC Santa Barbara.



# Abstract

The aim of this thesis is to investigate the factors affecting the interannual variability of the Belg rain in Ethiopia, in addition to see in which degree the NorESM can capture these factors. A significant connection was found between Belg rain and five ocean regions: Agulhas current, the northern and southern patch of the PMM, Benguela Niño, and the Indian Ocean. There was also found a connection between Belg rainfall in Ethiopia and a negative NAO index and La Niña events. The results showed that the wind pattern over the Indian Ocean is a large contributor, in addition to the Subtropical Westerly Jet. The weather in Ethiopia is highly variable, and capturing this variability has been a major challenge. Investigating the factors causing interannual variability is an important step in improving seasonal predictions and climate services. These predictions can contribute to warning systems in case of extreme events, which is important due to Ethiopia's dependence on agriculture.



# Contents

<b>Acknowledgements</b>	<b>i</b>
<b>Abstract</b>	<b>iii</b>
<b>1 Introduction</b>	<b>1</b>
1.1 Aim of this thesis . . . . .	2
<b>2 Background</b>	<b>5</b>
2.1 Topography in Ethiopia . . . . .	5
2.2 Intertropical convergence zone . . . . .	6
2.3 Ocean and atmosphere phenomena . . . . .	7
2.4 Research done on MAM rainfall in Ethiopia . . . . .	10
<b>3 Methods</b>	<b>15</b>
3.1 Data . . . . .	15
3.2 Models . . . . .	17
3.2.1 NorESM2-MM . . . . .	17
3.2.2 NorCPM . . . . .	18
3.3 Statistical Methods . . . . .	19
<b>4 Results and Discussion</b>	<b>21</b>
4.1 Selecting study area and timing of the Belg season . . . . .	21
4.2 Choosing the base for composites . . . . .	22
4.3 Observation analysis . . . . .	23
4.3.1 850hPa Wind . . . . .	24
4.3.2 200hPa Wind . . . . .	25
4.3.3 SST teleconnections . . . . .	26
4.3.4 ENSO . . . . .	32
4.3.5 NAO . . . . .	33
4.4 NorCPM . . . . .	35
4.5 NorESM2-MM . . . . .	37
4.6 NorESM2-MM - analysis . . . . .	41
4.6.1 Wind 850 hPa - NorESM2-MM . . . . .	41
4.6.2 Wind 200 hPa - NorESM2-MM . . . . .	42
4.6.3 SST - NorESM2-MM . . . . .	44
4.6.4 NAO - NorESM2-MM . . . . .	44
4.7 Discussion . . . . .	45

<b>5</b>	<b>Conclusions and Future Work</b>	<b>49</b>
<b>A</b>	<b>Some appendix</b>	<b>51</b>



# List of Figures

- 2.1 Altitude distribution in Ethiopia. The green color represents lowlands while the orange color represents highlands. The figure is from a study by Asefa et al. (2020). . . . . 6
- 2.2 Schematic view of the Walker circulation (Wright et al., 1983) . . . . . 9
- 4.1 Left panel (a) shows an overview of MAM precipitation divided by annual mean over Ethiopia. The blue (red) color indicates where MAM precipitation is larger(less) than the annual mean. The shaded area represents where the values are larger than 2. The right panel shows a histogram with precipitation amount (mm/month) for each month in the shaded area in figure a. . . . . 22
- 4.2 Left panel (a) shows an overview of FMAM precipitation divided by annual mean over Ethiopia. The blue (red) color indicates where FMAM precipitation is larger(less) than the annual mean. The shaded area represents where the values are larger than 1,5. The right panel shows a histogram with precipitation amount (mm/month) for each month in the shaded area in figure a. . . . . 22
- 4.3 A time series of the MAM precipitation [mm/month] in the Belg-dominated area for ERA5 (yellow line) and CHIRPS (green line) from 1981-2021. The corresponding straight line represents the standard deviation. . . . . 23
- 4.4 MAM mean 850 hPa wind [m/s]. The arrows indicate the wind anomaly's direction and strength, and the contour shading represents the wind strength. . . . . 24
- 4.5 MAM wind anomaly [m/s] at 850hPa for wet events (upper figure(a)) and dry events (lower figure (b)). The arrows indicate the wind anomaly's direction and strength. Black arrows indicate values that are significant at the 10% significance level. Grey arrows indicate non-significant values. The contour shading represents specific humidity [kg/kg] anomalies, also at 850hPa height. The blue shading indicates values wetter than climatology, and the red shading indicates drier than climatology. . . . . 25
- 4.6 MAM mean 200 hPa wind [m/s]. The arrows indicate the wind anomaly's direction and strength, and the contour shading represents the wind strength. . . . . 26

- 4.7 MAM wind anomaly [m/s] at 200hPa for wet events (upper figure(a)) and dry events (lower figure (b)). The arrows indicate the wind anomaly's direction and strength. Black arrows indicate values that are significant at the 10% significance level. Grey arrows indicate non-significant values. The contour shading represents specific humidity [kg/kg] anomalies, also at 200hPa height. The blue shading indicates values wetter than climatology, and the red shading indicates drier than climatology. . . . . 27
- 4.8 Correlation between MAM precipitation in the Belg domain and MAM SST. The red color indicates a positive correlation, while the blue color indicates a negative correlation. The shaded area corresponds to where the correlations are significant at the 10% significance level. The boxes indicate areas with a high correlation that will be investigated further. . 27
- 4.9 Correlation between MAM precipitation in the Belg domain and March SST over the Indian Ocean. The red color indicates a positive correlation, while the blue color indicates a negative correlation. The shaded area corresponds to where the correlations are significant at the 10% significance level. The box indicates the western Indian Ocean area with a high positive correlation that will be investigated further. . . 28
- 4.10 Overview of the correlation between MAM precipitation in the Belg domain and SST in the 5 regions Benguela, Agulhas, PMM-north, PMM-south, and the Indian Ocean for each month. The months indicated with t=0 represent SST in the months the same year as the MAM season are correlated, while months with t=-1 indicate that SST the year before the MAM season is correlated. A circle indicates values where the correlations are significant at the 10% significance level. . . . 29
- 4.11 Correlation between MAM SST in the Agulhas region and MAM wind in V-direction at 850 hPa. The red color indicates a positive correlation, while the blue color indicates a negative correlation. The shaded area corresponds to where the correlations are significant at the 10% significance level. . . . . 31
- 4.12 MAM mean sea level pressure anomaly [Pa] at for dry events (figure a) and wet events (figure b). The blue shading indicates negative pressure anomaly, and the red shading indicates positive pressure anomaly. . . . 31
- 4.13 Left panel: Correlation between MAM SST in the northern PMM patch and MAM wind in U-direction at 850 hPa. Right panel: same as the left one but for the southern PMM patch. The red color indicates a positive correlation, while the blue color indicates a negative correlation. The shaded area corresponds to where the correlations are significant at the 10% significance level. . . . . 32
- 4.14 MAM precipitation [mm/month] anomaly over Ethiopia for cold ENSO events (left figure(a)) and warm ENSO events (right figure (b)). The blue shading indicates more precipitation than climatology, and the red shading indicates less precipitation than climatology. . . . . 34

4.15	MAM geopotential height [m] (850hPa) anomaly for wet events (left figure(a)) and dry events (right figure (b)). The red shading indicates a larger geopotential height than climatology, and the blue shading indicates a lower geopotential height than climatology. . . . .	34
4.16	Left panel represents the first EOF of the mean sea level pressure over the Atlantic Ocean. The color bar represents explained variability by the first EOF. The figure to the right represents the corresponding principal component. . . . .	35
4.17	MAM precipitation[mm/month] anomaly over Ethiopia for years with negative NAO index (left figure(a)) and positive NAO index(right figure (b)). The blue shading indicates more precipitation than climatology, and the red shading indicates less precipitation than climatology. . . . .	36
4.18	An overview of MAM precipitation divided by annual mean over Ethiopia from the NorCPM. The ensemble mean from all 30 ensemble members was used in this calculation. The blue (red) color indicates where MAM precipitation is larger(less) than the annual mean. . . . .	36
4.19	Histogram with precipitation[mm/month] amount for each month in northern and southern Ethiopia in the boxes selected in Figure 4.18. The left panel shows a histogram for the northern box, and the right panel shows the southern box. The histograms are based on the ensemble mean of the 30 available ensemble members. . . . .	37
4.20	Topography[m] distribution used in NorCPM in Ethiopia. Green color represents lowlands while orange represents highlands. . . . .	37
4.21	An overview of MAM precipitation divided by annual mean over Ethiopia from the NorESM2-MM for two periods and individually for each ensemble member. The shaded area illustrates where the MAM precipitation is significantly larger than the annual mean, so when the MAM/annual means is larger than the threshold value under each figure. The upper panel shows the calculation for 1981-2014, while the bottom panel shows the calculation for the entire available time period (1850-2014). The figures to the left are for ensemble member 1, the central represents ensemble member 2, and the right figures are for ensemble member 3. The blue (red) color indicates where MAM precipitation is larger(less) than the annual mean. . . . .	38
4.22	The figure shows an overview of NorESM2-MM MAM precipitation divided by annual mean over Ethiopia. The calculation used the ensemble mean of all three ensemble members from 1850 to 2014. The blue (red) color indicates where MAM precipitation is larger(less) than the annual mean. The shaded area represents where the values are larger than 1.9. . . . .	39
4.23	histogram with precipitation[mm/month] amount for each month and every ensemble member in the shaded area in Figure 4.22. The red bar shows the result for ensemble member 1, yellow for ensemble member 2, and green for ensemble member 3. The blue line represents the ensemble mean of the three members. . . . .	39

4.24	A time series of the MAM precipitation [mm/month] in the Belg-dominated area (shaded area in Figure 4.22) for ensemble member 1 (magenta), ensemble member 2 (yellow) and ensemble member 3 (blue) from 1981-2014. The corresponding straight lines represent the standard deviation. . . . .	40
4.25	Topography[m] distribution used in NorESM2-MM in Ethiopia. Green color represents lowlands while orange represents highlands. . . . .	41
4.26	MAM wind [m/s] (850hPa) anomaly from three ensemble members of the NorESM2-MM. Dry events are shown to the left, and wet events are shown to the right. The arrows indicate the wind anomaly direction and strength. Black arrows indicate values that are significant at the 10% significance level. Grey arrows indicate non-significant values. The contour shading represents specific humidity [kg/kg] anomalies, also at 850hPa height. The blue shading indicates values wetter than climatology, and the red shading indicates drier than climatology. . . . .	42
4.27	MAM wind [m/s] (200hPa) anomaly from three ensemble members of the NorESM2-MM. Dry events are shown to the left, and wet events are shown to the right. The arrows indicate the wind anomaly direction and strength. Black arrows indicate values that are significant at the 10% significance level. Grey arrows indicate non-significant values. The contour shading represents specific humidity anomalies at 200 hPa [kg/kg]. The blue shading indicates values wetter than climatology, and the red shading indicates drier than climatology. . . . .	43
4.28	Correlation between MAM precipitation in the Belg domain and MAM surface temperature. Both variables are from the NorESM2-MM. The red color indicates a positive correlation, while the blue indicates a negative one. The shaded area corresponds to where the correlations are significant at the 10% significance level . . . . .	44
4.29	MAM geopotential height [m] (850hPa) anomaly from three ensemble members of the NorESM2-MM. Dry events are shown in the upper panel, and wet events are shown in the bottom panel. The red shading indicates a larger geopotential height than climatology, and the blue shading indicates a lower geopotential height than climatology . . . . .	45
A.1	The figure shows an overview of ERA5 MAM precipitation divided by annual mean over Ethiopia. The blue (red) color indicates where MAM precipitation is larger (less) than the annual mean. The shaded area represents where the values are larger than 2. . . . .	51
A.2	Correlation between MAM precipitation in the Belg domain and MAM wind in U-direction at 850 hPa. The red color indicates a positive correlation, while the blue color indicates a negative correlation. The shaded area corresponds to where the correlations are significant at the 10% significance level. . . . .	51

- 
- A.3 Correlation between MAM precipitation in the Belg domain and MAM wind in U-direction at 200 hPa. The red color indicates a positive correlation, while the blue color indicates a negative correlation. The shaded area corresponds to where the correlations are significant at the 10% significance level. . . . . 52
- A.4 SST composite from the dry and wet events in the Belg-dominated area. The values are anomalies from the climatology where red color indicates warmer than climatology and blue indicates colder. on. The dots indicate where the correlations are significant at the 10% significance level . . . . . 52



# Chapter 1

## Introduction

Several African countries have less high-quality data and a lack of research capacity compared to the other continents. Therefore, fewer climate studies exist for these regions (Shongwe et al., 2011), and Ethiopia is no exception. My thesis will contribute to this knowledge gap in investigating the Ethiopian rainfall regime that takes place during spring.

Ethiopia has a complex topography located in the eastern part of Africa. During the 1970s and 1980s, Ethiopia was one of the poorest countries in the world, but its economy began to grow in the mid-1990s (Shiferaw et al., 2017). The poverty rate in Ethiopia was reduced from 48% in 1990 to 23.5%, which is one of the largest declines in extreme poverty in Sub-Saharan Africa (Woldehanna et al., 2022). However, the country's biggest challenge is keeping the economy stable (Shiferaw et al., 2017). Rain-fed agriculture plays the biggest role in the country's economy and has, therefore, a large impact on the livelihood of its population. Small changes in precipitation patterns can have consequences for the population. Grey and Sadoff (2007) showed a significant relationship between rainfall variability and the gross domestic product.

At the same time, the region has experienced several episodes of extreme events like drought and flood. With global warming, we can expect an increase in these extreme events in east Africa (Tan et al., 2020). Omondi et al. (2014) showed that the overall trend is a reduction in precipitation and an increase in periods of drought. With this trend and its relation to the economy, Bryan et al. (2013) predicted that the critical staple crops in Africa will decline by 8-22% by 2050 due to climate change. This will significantly affect a country like Ethiopia, which is sensitive to changes in agriculture. An example of the impact of severe drought is the drought in 2002, where 14.2 million people were affected (20% of the country's population) (Bank, 2007). In 2022, a sequence of five sequential droughts led to several crises in the Horn Of Africa related to food and fuel prices. The drought in 2022 was the driest on record, which led to widespread starvation (Funk et al., 2023), and 2023 does not seem to be any better as it has been announced already that immediate global action is required to prevent famine in the Horn of Africa (ICPAC, 2022). Understanding the factors influencing the interannual variability of the Belg rain is needed to predict extreme events better and

develop disaster preparedness, procedures, and city planning.

There are three rainfall regimes in Ethiopia. Kiremt is the dominating season in the northern part of the country and takes place in June-September. The primary rainfall season over the southern part of Ethiopia is the Belg season which takes place in the spring and lasts from March to May (MAM). There is also a rainy season in October-December that is most visible in the southern part but not as significant a contributor as the MAM season (Bekele-Biratu et al., 2018).

The impact of the Belg rainfall varies depending on the area, but the Belg season is the most significant contributor to precipitation in the southern part of Ethiopia. It also has impacts in terms of agriculture in other regions. Rainfall during the Belg season will impact crop performance during the summer rain due to soil moisture availability. A wet Belg season will lead to greater moisture availability and facilitate early planting of long-duration varieties of the leading food crops (Gummadi et al., 2018). The Belg season is the most important in southern Ethiopia, but also very important in the northern (and central) parts of Ethiopia, where the Kiremt season dominates.

Modern seasonal to inter-annual predictions are in high demand because many activities are influenced by climate variability to a certain degree (Takele et al., 2020). However, the idea that the climate can be predictable might be hard to understand given that the weather is highly affected by randomness and can only be predicted a few days in advance. On a seasonal scale, the errors become so large that it becomes more like a wild guess, one may think. However, there is some information to be uncovered based on different sources of predictability (Hansen et al., 2011). Knowing the controlling factors for a specific weather regime can help us predict extreme events several months in advance. These factors will be investigated in this thesis, which will contribute in improving seasonal forecasts of the Belg rain in Ethiopia. A way of making a seasonal prediction is using climate models. However, for the models to make a correct prediction, the model have to be able to resemble these factors as well.

Some work has been done investigating the Kiremt season (e.g. Gleixner et al. (2017)), but there has not been nearly as much work done on investigating the factors causing interannual variability in the Belg season compared to Kiremt. There is also some disagreement about which factors are important here. Thereby, this thesis will contribute to this knowledge gap.

## **1.1 Aim of this thesis**

The aim of this thesis is to investigate which factors that are influencing the interannual variability of Belg rain in Ethiopia. To do this, I wanted to see what the climate system looks like in situations with a wet and dry Belg season. To do this, I used precipitation



data from CHIRPS, SST data from NOAA, and wind and geopotential height from ERA5. I also calculated the correlation between Belg rain and different climatic factors and see if there were any connections. Knowing what the climate system looks like in situations with a wet and dry Belg season can help us predict the intensity and timing of the season. Information about this can be used in predictions that can help us predict extreme drought and flood in Ethiopia, which is crucial due to their rural conditions and dependence on agriculture. Lastly, this thesis aims to investigate if these conditions are visible in the output of NorCPM and NorESM2-MM and if they can reproduce the precipitation pattern in Ethiopia.



# Chapter 2

## Background

This section will cover the background information needed in order to investigate the interannual variability of MAM precipitation in Ethiopia. The first section will cover some information regarding Ethiopian topography. This is important to understand since the country has a complex topography that has a large impact on the precipitation distribution. Secondly, this section will cover the Intertropical Convergence Zone, which is the reason why there are two rainy seasons in the southern part of Ethiopia and one in the north. Lastly, the chapter will cover some terminology and an overview of the research done on this topic.

### 2.1 Topography in Ethiopia

There are mainly three ways topography can affect regional weather patterns. The topography can intensify the solar heating over land by providing an elevated heat source which magnifies the land-sea temperature contrast. This may facilitate the monsoon regimes that produce convective rainfall. The second factor is orographic precipitation where moist air is forced up toward the slope of the mountain where the air cools, moisture condenses and rainfall is created in addition to latent heat. Lastly, topographic barriers in the tropics can obstruct the large-scale airflow and force some air to go around, instead of over the topography. This may set up a large-scale circulation that extends into the extra tropics through planetary waves (Meehl, 1992).

Enyew and Steeneveld (2014) analyzed the impact topography has on the regional weather systems and flooding in Ethiopia. The results here showed that changing the topography had large consequences for the spatial precipitation pattern, which got a clear reduction and was shifted when reducing the orographic effect. The study concludes that topographic barriers play an important role in the precipitation amount and distribution in the region. Therefore, it is important to have an overview of the topography in Ethiopia when investigating the precipitation pattern.

A complex topography characterizes Ethiopia. The country's highlands are known as "the roof of Africa" since the majority of land in Africa over 3000m is located in

Ethiopia. The area is extremely heterogeneous with high mountains and deep valleys (Roberts et al., 2012). Figure 2.1 is from a study done by Asefa et al. (2020) and shows the variety in topography the country is affected by. The southern part of the country has an overall low altitude, while the highlands dominate in the northern and central parts of the country.

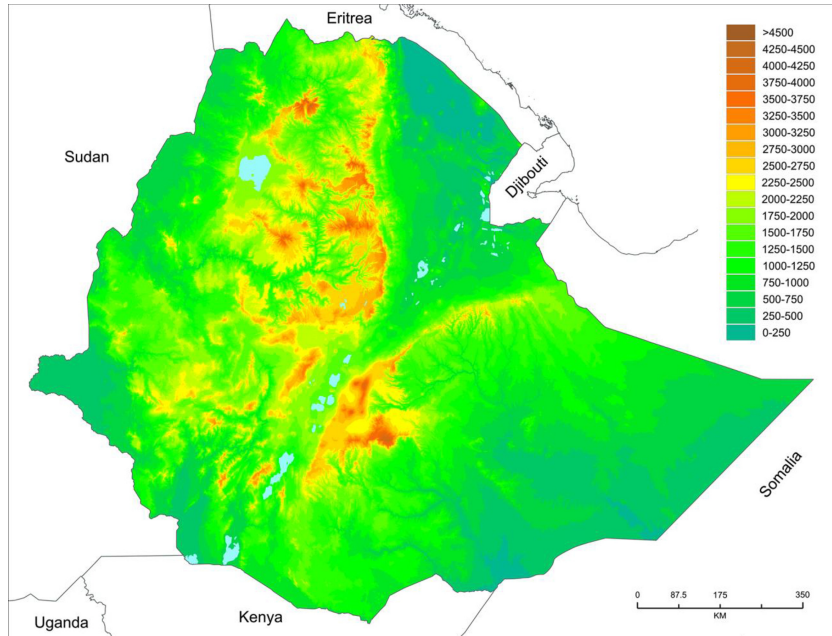


Figure 2.1: Altitude distribution in Ethiopia. The green color represents lowlands while the orange color represents highlands. The figure is from a study by Asefa et al. (2020).

## 2.2 Intertropical convergence zone

Ethiopian rainfall is primarily governed by the movement of the Intertropical convergence zone (ITCZ) (Sutcliffe et al., 1999). This convergence zone is an east-west-oriented low-pressure "belt" near the equator. The surface northeast and southeast trade winds converge in this region, and moist air is forced upward, producing high clouds and precipitation. Thereby the regions in this zone are affected by heavy rainfall in the period the convergence zone is passing (Oliver, 2008). In addition, the sea surface temperature (SST) in this area rises due to the direct sunlight from the sun nearly above the equator. The increase in SST leads to convection in the tropics which is responsible for the ITCZ and the upward branch of the Hadley cell (Rasmusson and Arkin, 1993).

The location of the ITCZ varies with season, but it is usually found within 350 km from the equator (varying between 5° north and south). The zone is usually where the most intense solar heating takes place. Therefore, the convergence zone moves north and south, and some regions get a "double ITCZ" and a bi-modal rainfall pattern. (Oliver, 2008).

In the southern and southeastern parts of Ethiopia, the ITCZ passes two times which results in a bi-modal pattern. This bi-modal pattern results in a rainy season in March-May when the convergence zone travels north, and another rainy season when the zone migrates south in September-November. In the northern and western parts of Ethiopia, the ITCZ only covers the region one time, which results in a mono-modal rainfall regime with a dominating rainy season in June-September (Sutcliffe et al., 1999).

Based on the movement of the ITCZ, Ethiopia can roughly be divided into three climatic regions. One region covers central, northeastern, and parts of eastern Ethiopia. This region has a dry period from October-February, a short rainy season from March-May (often referred to as the Belg season), and a long rainy season from June to September. The second region is located in the northwestern and western parts of Ethiopia. This region is characterized by a long rainy season extending from March to November with most of the rainfall coming in the dominating rainy season in June-September. The third and last region is located in Ethiopia's southern and southeastern parts. This season is affected by two rainy seasons: one from March-May and one from September-November (Gizaw et al., 2017). This last region will be the main focus in this thesis.

## 2.3 Ocean and atmosphere phenomena

In the result section of this thesis, several areas/phenomena stand out as factors that affect the interannual variability of Belg rain in Ethiopia. This section will explain those phenomena.

The North Atlantic Oscillation (NAO) is the most prominent pattern of atmospheric variability over the mid-, and high latitudes in the northern hemisphere. This index is based on the pressure difference between the Subtropical High over the Azores and the Subpolar Low over Iceland and is most dominant during November-April. The NAO signal is referred to as a redistribution of atmospheric mass between the Arctic and the subtropical Atlantic. When the NAO changes sign and go from one phase to another, it can produce large changes in the wind pattern over the Atlantic, which also affects the heat and moisture transport in the area (Hurrell et al., 2003). Even though the NAO index greatly impacts the surrounding weather systems, the index has seemed to be largely unpredictable. This was until recently since later studies have shown that the index is more predictable than many thought (Smith et al., 2020).

Another atmospheric circulation pattern is the Walker circulation, which describes the large-scale atmospheric circulation along the longitude-height plane along the equatorial Pacific Ocean. Low-level easterly winds across the central Pacific, rising air over the warm western Pacific, sinking motion over the colder eastern Pacific, and westerly upper troposphere winds represent this circulation pattern. They are shown in Figure 2.2. The figure shows that a secondary circulation is also included in the

Walker Circulation. This circulation includes rising air over South America and Africa, compensating sinking air over the Atlantic and Indian oceans. In addition to weaker vertical motion, these cells are smaller than the main Walker cell. Like the main Walker cell, these cells also drive horizontal winds at the surface, and upper troposphere showed in Figure 2.2. For instance, it results in a low-level westerly wind and upper-level easterly wind over the Indian Ocean. However, several factors can affect the Walker circulation and thereby control the wind systems in the entire Tropics. One example is during an El Niño or a La Niña event. During such an event, the position and velocity of the rising air may change according to where the high SST values are, so an El Niño event will weaken the Walker Circulation, while a La Niña will strengthen this circulation (Lau and Yang, 2003).

El Niño-Southern Oscillation (ENSO) is the largest climate signal on an interannual time scale. Every three to seven years, we often observe a pronounced warming of the tropical Pacific ocean. This warming is visible from the International Dateline to the west coast of South America and greatly impacts the local and global climate. This warming phase is known as El Niño, while the cold phase is known as La Niña (Trenberth, 1997). Earlier, El Niño was referred to as the unusual appearance of warm water off the coast of Peru around Christmas time. Still, later by Bjerknes (1969) the term has become synonymous with basin-wide phenomena (Trenberth, 2020). Several indices exist for ENSO events, but El Niño and La Niña events are most commonly defined as when the Niño3.4 value exceeds a threshold (e.g. above and below  $0.5^{\circ}\text{C}$ ). Values that don't exceed these are considered neutral (Trenberth, 1997). ENSO peaks in the boreal winter, traditionally defined as December-February (Haszpra et al., 2020).

ENSO is also linked to several teleconnections in the atmosphere and ocean. Teleconnections are linkages across large distances, and signify that there is a physical reason for the simultaneous variations. Teleconnections can occur through the ocean or atmosphere, although the primary reason is the presence of Rossby waves in the atmosphere (Trenberth, 2020). The teleconnections related to ENSO are important to understand for several reasons. Because ENSO can affect climate in areas far away, ENSO SST anomalies can be used to forecast on a seasonal or annual time scale (Sterl et al., 2007).

Farther north of the ENSO pattern, we find another important statistical mode of climate variability in the Pacific Ocean, which is the Pacific Meridional Mode (PMM). The PMM is a coupled SST-surface wind pattern located in the northeastern part of the Pacific. This pattern has been proposed to largely originate from stochastic atmospheric forcing in the mid-latitudes (Di Lorenzo et al., 2015). The PMM pattern is most visible in the spring (January-May) Chang et al. (2007). According to several studies (e.g. Di Lorenzo et al. (2015), Chang et al. (2007)), the PMM can affect ENSO variability, and the two patterns together can induce decadal variability in the Pacific.

Similar to ENSO, PMM is also connected to several teleconnection systems. The PMM

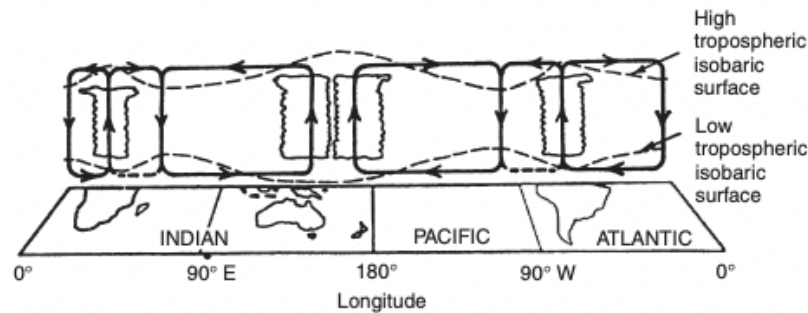


Figure 2.2: Schematic view of the Walker circulation (Wright et al., 1983)

decreases the zonal Walker circulation over the Pacific Ocean. The weakening of the Walker circulation affects the low-level westerlies over the Indian Ocean. The positive phase of the PMM results in weaker westerlies at 850 hPa (Hari et al., 2022). The PMM pattern has also been proven to be useful in seasonal prediction for different regions several times (e.g. Zhang et al. (2019), Promchote et al. (2018)).

There are also several oscillation systems in the Atlantic Ocean. One of the most productive marine ecosystems in the world is the Angola Benguela upwelling system located in the southeast of the tropical Atlantic Ocean (Chavez and Messié, 2009). This region is recognized by the presence of a sharp meridional temperature gradient called the Angola Benguela front (ABF). The temperature gradient is where the warm tropical water masses in the north meet the cold upwelled water in the south. Similar to the ENSO pattern, SST variability in this region is characterized by warm phases (Benguela Niño) and cold phases (Benguela Niña). These warm and cold events peak in the spring (March-April) (Rouault et al., 2007). These cases can have a large impact on the surrounding areas. Benguela Niños often lead to floods in Angola and Namibia, in addition to increased rainfall over the Namib desert (e.g. (Rouault et al., 2003) (Hansingo and Reason, 2009)). On the other hand, droughts over the Angola Benguela region are often connected to a Benguela Niña event (Koseki and Imbol Koungue, 2021).

Lastly, investigating the Indian Ocean, we find the Agulhas current, which is the strongest western boundary current in the southern hemisphere and is located near the southern tip of Africa. Throughout the year, the current releases a lot of heat into the atmosphere above (Zinke et al., 2014). The weather in the surrounding land areas may be affected by the Agulhas current. Several studies have shown that the Agulhas current can induce weather systems under certain atmospheric conditions. For instance, the Agulhas SST front can enhance storm-track activity and reinforce the Mascarene high through the net dynamical forcing of the storm-track activity on the mean flow Miyamoto et al. (2022).

## 2.4 Research done on MAM rainfall in Ethiopia

The aim of this thesis is to investigate the interannual variability of the Belg rainfall in Ethiopia. Belg rainfall turns out to be highly variable over most regions in Ethiopia with an annual rainfall variation between 15-55%. However, the variability decrease in the southern part of the country (which is the main focus in this thesis) where it becomes between 16-30%. In this region, nearly 80% of the rainfall comes during the MAM season (approximately 400 mm/year). The Belg season has shown a significant decline in rainfall amount over the last years. The largest decline is along the rift valley, which is a region where Belg season makes a significant contribution to the annual rainfall. During the last 31 years a decline of 50-150 mm have been observed during the MAM season. Even though there is a decline in seasonal rainfall during MAM, there is an increase in extreme rainfall (Gummadi et al., 2018).

In order to improve preparedness for these extreme events, the factors influencing the interannual variability of MAM precipitation are important to understand and predict. Jury (2015) investigated climatic determinants for MAM rainfall in southeast Ethiopia. Correlation maps and composites analysis on wet and dry seasons was carried out to study these relations. The results showed a relation between MAM rainfall in southeastern Ethiopia and Benguela Niño in the southeastern Atlantic. A cold Benguela Niño (upwelling) creates a cold plume that sweeps north into the Gulf of Guinea and damps the convection. This sets up a velocity potential gradient across the central African monsoon, causing it to expand towards the southeast in Ethiopia. This influence affects the MAM precipitation at an interannual scale. The study also showed that the Indian ocean plays a key role in MAM precipitation in Ethiopia at an intra-seasonal timescale. Easterly winds from the Indian Ocean rise towards southeast Ethiopia and converge with westerlies from the Congo basin. Analyses of 200hPa westerly flow over the central Atlantic suggest influence by ENSO. If a strong ENSO signal persists into the spring, the MAM precipitation may be affected.

Williams and Kniveton (2011) also investigated the factors controlling spring precipitation in Ethiopia. To research this the country was divided into five homogeneous rainfall zones. The zones were chosen by using two steps. The first was to see where rain gauges in the area showed similar annual cycles. Afterward, correlation both within and across the zones was done, and boundaries were adjusted, so the interstation correlation within each zone was higher than the mean. The data used was ERA-40 re-analyses covering 1969-2001, and they defined the season to start in February and end in May.

When investigating FMAM precipitation in Ethiopia Williams and Kniveton (2011) found 5 factors that control the Belg season. The first factor is related to the Subtropical Westerly Jet (STWJ). A stronger and southward shift of the jet affects the Belg season due to the trough and convection associated with the jet. The second factor the study shows is the relation to ENSO. A warm ENSO creates stationary Rossby waves which



propagate east and north entering the subtropical westerly jet in the Atlantic and reaching North Africa. This teleconnection between ENSO and Rossby waves and the subtropical westerly jet was also shown by Shaman and Tziperman (2005) when investigating the effect ENSO had on the Tibetan Plateau snow depth. A southward shift in the subtropical westerly jet is associated with a wet Belg. The Rossby waves from a warm ENSO make the jet travel further north, and the jet brings moisture too far north to reach Ethiopia. However, there are some disagreements on the effect ENSO has on the MAM rainfall. Hoell et al. (2014) investigated this relationship for entire East Africa. The results showed that a La Niña episode could either increase or decrease MAM rainfall in East Africa. This depends on the characteristics of the episode. A La Niña with cold anomalies in the central and eastern Pacific and neutral conditions in the western Pacific tend to produce a positive anomaly in MAM rainfall. On the other hand, a weaker anomaly in the eastern and central Pacific, but warm anomalies in the western Pacific tend to have the opposite effect and lead to a negative MAM rainfall anomaly over eastern Africa. However, several studies done on this teleconnection did not show any significant correlation between spring rainfall in East Africa and ENSO (e.g. Ogallo (1988), Hastenrath et al. (1993), Phillips and McIntyre (2000)).

According to Williams and Kniveton (2011), a third factor affecting the Belg season is the North Atlantic Oscillation (NAO). A negative NAO means a weaker Azores High, and the mid-latitude depressions can propagate via the Mediterranean and displace the Arabian high to the south. A southward shift in the Arabian high leads to easterlies bringing moisture towards Ethiopia, leading to enhanced precipitation. Another factor controlling the rainy season, according to Williams and Kniveton (2011) is an easterly anomaly from the Indian ocean. These easterlies are associated with the Arabian high, which is associated with the Azores high and the NAO. A negative phase of the NAO leads to a weaker Azores high and a stronger Arabian high which leads to stronger easterly anomalies from the Indian ocean. These anomalies bring moisture over Ethiopia and lead to wet seasons. The last thing the study brings up is the effect of tropical cyclones. Less frequent tropical cyclones over the southwest Indian ocean will lead to a wetter Belg season through the diversion of moisture to the cyclone region. This effect was also described by Shanko and Camberlin (1998).

Beyene et al. (2022) also divided Ethiopia into different parts based on the precipitation pattern while looking at the long rains. This study researched teleconnections between climate indices and precipitation anomaly using wavelet coherence and correlation analysis. Ethiopia was divided into five zones based on where the precipitation pattern is homogenous. The zones representing the Belg dominating area (southeast Ethiopia) in this study are cluster 4 and partly cluster 3. The study found a strong connection between the Indian Ocean dipole and precipitation anomaly in southeast Ethiopia. A strong teleconnection between Nino 3.4 and precipitation anomalies in the same area was also found. The connection between North Atlantic Oscillation (NAO) and precipitation anomalies was also investigated. However, it is a less effective climate index than others, especially in the southeastern part of Ethiopia. The connection with Nino 3.4 and the Indian ocean dipole positively correlates with precipitation anomalies

of southeast Ethiopia, while NAO shows a weak negative correlation. In which way these indices affect the precipitation in Ethiopia was not discussed.

The influence of Pacific SST and the Somali Jet on spring precipitation in Addis Ababa (Ethiopia) was investigated by Eden et al. (2014). A linear relationship between Ethiopian spring rainfall and basin-wide Pacific SST. The correlation pattern has a tripole structure that resembles ENSO and PDO. However, the pattern describes links independent of ENSO and PDO since these are only weakly correlated with precipitation in Ethiopia. The study also describes the connection with the Somali Jet and that this connection exists when we have an early development of the jet.

Camberlin and Philippon (2002) studied the East African March-May rainy season and the associated atmospheric dynamics. The regions investigated in this study were Kenya, Uganda and Ethiopia by doing composite analysis. The different months were researched individually due to several studies showing that the Long Rains in the spring are characterized by inhomogeneity (e.g. Zorita and Tilya (2002)). In other words, the factors controlling precipitation vary from month to month (MAM). However, for Ethiopia, according to Camberlin and Philippon (2002), there were similar atmospheric anomaly patterns between the composites for March, April, and (to a lesser extent) May. This pattern corresponds to a southerly extension of the subtropical westerly jet which decreases the wind strength at approximately 30°N. Divergence ahead of the trough will likely induce upward motion and more rain in Ethiopia. The results here showed an anticyclonic feature over the central Mediterranean, a cyclonic part over the Red Sea, and waves with a tilt towards the northeast. The abnormal high over the Arabian sea increases northeasterly winds near the tip of the Horn of Africa. This increase in wind strength advects moist air towards Ethiopia.

Alhamsry et al. (2019) was investigating seasonal Rainfall Variability in Ethiopia and Its Long-Term Link to Global Sea Surface Temperatures were researched. The method of cross-correlation between SST and precipitation in both the northern (summer rainfall region) and southern (spring rainfall region) part of Ethiopia was used in this paper. The results for the spring season showed a significant and high correlation between spring rainfall and SST in the northern Atlantic (with a lag time of 6-7 months). A strong correlation was also found between spring rainfall and SST in two regions in the southern Indian Ocean (with a lag time of 7-8 months). The study concludes that these regions can effectively be inputs for Ethiopian spring rainfall prediction models.

Overall the research done on the Belg season has a large spread in the results and there are some disagreements between the different studies. In general, there is still uncertainty about which factors control the MAM precipitation in Ethiopia. The disagreement among scientists is primarily related to the role ENSO, NAO, and the Indian Ocean and their connection to MAM precipitation in Ethiopia. These are among

the others factors I will investigate in my thesis.



# Chapter 3

## Methods

This chapter will include a description of the different observational data used in this thesis and an overview of some of the evaluations done on these data sets. Secondly, I will present a description of the different models I used in this thesis in addition to some evaluation on these to see what the models simulate well and what they struggle with. Lastly, an overview of the different statistical methods used in this thesis follows.

### 3.1 Data

In order to investigate long-term climate conditions, observational data are necessary. These mainly come from three sources: in situ measurements, satellites, and model estimates based on the laws of physics, such as reanalysis products (Lavers et al., 2022). In this master's thesis, I have looked at the following variables: Precipitation, Sea Surface Temperature (SST), wind (850hPa height, and 200hPa height), geopotential height, and mean sea level pressure. All of these are observations from a mix of the aforementioned sources. All of the observational data in this thesis is detrended to remove the effects of global warming. This is useful in my thesis to distinguish trends from variability when investigating the Belg rainfall in Ethiopia.

Monthly SST data for this thesis were obtained from NOAA Optimum Interpolation (OI) Sea Surface Temperature (SST) V2. The data is global (89.5N - 89.5S, 0.5E - 359.5E), from 1981 to the present (downloaded in 2020). The data has a resolution of 1.0-degree latitude x 1.0-degree longitude. The data is achieved by combining in situ and satellite-derived SST data (Hurrell et al., 2008). The advantage of this blending does is that the satellite data is uncertain, so the in situ data can make corrections to reduce the uncertainty. The monthly fields are derived linearly interpolating the weekly OI fields to daily fields, before averaging the daily values over a month (Reynolds et al., 2002).

A disadvantage of combining these products is the decrease in spatial resolution (Hurrell et al., 2008). In my thesis, I will look at large-scale processes, for which the resolution is sufficient. The accuracy of the data and the high spatial coverage

combined with the fact that the data is easily accessible and regularly updated make the NOAA OI SST V2 a good choice for this thesis.

Climate Hazards Group InfraRed Precipitation with Station data (CHIRPS) was used to examine precipitation. The data builds on approaches used in thermal infrared precipitation products. The Tropical Rainfall Measuring Mission Multi Satellite Precipitation Analysis version 7 was used to calibrate the global Cold Cloud Duration. CHIRPS also builds on state-of-the-science interpolated gauge products and uses a "smart interpolation" method. The data consists of monthly data from 1981 to the present (downloaded in 2021). The data spans the landmasses from 50°S-50°N, and for all longitudes. It has a high resolution of 0.05° latitude x 0.05° longitude. The high resolution in precipitation data is an advantage in this thesis since data will be used locally in Ethiopia. Due to the high resolution, the selection of the study area becomes more accurate (Funk et al., 2015).

Dinku et al. (2018) saw that the CHIRPS data perform especially well over Ethiopia. The study compared the CHIRPS, ARC2, and TAMSAT products over parts of eastern Africa to rain gauge data. Both regional and country level was evaluated in the period 2006 to 2010. A challenge for the study was that some available stations were also used in the CHIRPS product. Thus Dinku et al. only used stations located at least 25 km away from those used in CHIRPS. This was also the case for some stations in Ethiopia, but the measurements here were less affected compared to Tanzania and Kenya. Meanwhile, there was a lack of independent stations in the southern part of Ethiopia, making the evaluation more uncertain in this region. In total, 1200 stations spread across East Africa were used. The results from this study show that CHIRPS is closer to the observed station data compared to the ARC2 and TAMSAT2 which overestimates the coverage of the rainfall fields. Several other studies have done similar analyses to investigate the performance of CHIRPS in East Africa (e.g. Lemma et al. (2019), Muthoni et al. (2019)). These also support the results of Dinku et al. (2018).

For mean sea level pressure, wind, and geopotential height, I used ERA5. The data spans from 1980-2018. ERA5 is the latest ECMWF reanalysis and provides a comprehensive overview of the global atmosphere, land surface, and ocean waves. This system is based on Cy41r2 which was used in the ECMWF operational medium-range forecasting system from March 8th to November 21st, 2016. The reanalysis is based on the use of data assimilation (Hersbach et al., 2020).

Significant improvements have been made in the ten years between ERA-interim and ERA5. One improvement for the atmosphere assimilation is the radiation scheme used in ERA5 which is a major upgrade compared to the scheme used in ERA-interim. Another atmospheric improvement in the ERA5 is the large-scale cloud and precipitation scheme. This scheme was improved with a better representation of mixed-phase clouds and prognostic variables for snow and precipitation. There were

also improvements to the microphysics parameterizations. Changes in the convection parameterizations were also done by improving the entrainment and coupling with large-scale systems. This improvement was especially important in the tropics where the Hadley circulation causes convection. Several other improvements were made in the transition from ERA-interim to ERA5 which are further explained by Hersbach et al. (2020).

Lavers et al. (2022) evaluated ERA5 precipitation on a global level against station observations. Looking at extreme events the study showed that there are some limitations associated with the reanalysis. By investigating tropical cyclone Oswald in Australia, they saw that ERA5 struggled to resolve the convection and the following precipitation. They did the same to another storm in a mountain-dominated area in Europe. The results here showed that the reanalysis struggled to get the correct placement of the precipitation in the mountain-affected regions. The ERA5 has some challenges in representing the orographic enhancement of precipitation. In addition, the reanalysis shows too much precipitation on the leeward side of the mountain. The ability to represent orographic precipitation is very important in this study due to the fact that Ethiopia is a very mountain-dominated country and the topography has a large effect on the local weather and climate conditions (Smith, 1979).

Gleixner et al. (2020) also evaluated the performance of ERA5 over Africa by comparing it to observations. They analyzed near-surface temperature in addition to precipitation. The study performed an All-Africa, East African, and local evaluation. In the local evaluation, Ethiopia, Kenya, Uganda, and Tanzania were analyzed. The results for Ethiopia showed that ERA5 captured the precipitation seasonality well, but the amount was slightly different, as the reanalysis has a wet bias.

## 3.2 Models

In this thesis, I wanted to investigate to which degree the climate models NorESM2-MM and NorCPM can recreate the factors affecting interannual variability of Belg rain in Ethiopian. For the model results, the historical runs were used. In the first part of this study, I will use observation to see which climate signals control the interannual variability of spring rainfall in Ethiopia. In the second part, I want to see if these signals are visible in the climate models as well. An advantage of using climate models is that they consist several years compared to observational data used in this thesis.

### 3.2.1 NorESM2-MM

The Norwegian Earth System Model version 2 (NorESM2) will be used in this master thesis. The model was developed by the Norwegian Climate Center and is the second generation of the coupled Earth System Model. The Community Earth System Model

(CESM2.1) is the base of NorESM2. The NorESM2-MM has a  $1^\circ \times 1^\circ$  latitude-longitude resolution (Seland et al., 2020).

Makula and Zhou (2022) performed an evaluation on the performance of 43 CMIP6 models in reproducing annual cycle, climatology, and trend of observed precipitation over East Africa during 1950-2014. The results of this study showed that the NorESM2-MM generally overestimated the observed MAM precipitation over East Africa. The overestimation ranged from 30 to 60 mm/month. The results for NorESM2-MM showed that the model performs relatively well in estimating MAM precipitation in East Africa. In addition, the NorESM2-MM model captured the observed decreasing trend in MAM precipitation with a 90% confidence level.

### 3.2.2 NorCPM

In this thesis, I have used the Norwegian Climate prediction model (NorCPM). The output from NorCPM combines the Norwegian earth system model version 1 with an ensemble Kalman filter anomaly assimilation of SST and hydrographic profile observations. The model has a  $1.9^\circ \times 2.5^\circ$  latitude-longitude resolution (Bethke et al., 2021).

NorCPM stands out compared to other dynamical climate prediction systems by the use of its ensemble Kalman filter anomaly assimilation that performs cross-component ocean-to-sea-ice updates and its optimization for a vertical density coordinate. Using this scheme, the model can optimally use the observations by updating unobserved variables using known state-dependent relations. These relations also decrease shock by ensuring consistently updated variables (Bethke et al., 2021).

Bethke et al. (2021) also evaluated the NorCPM output. The results here showed that there is a mismatch between the model and observation on a grid scale. However, the model captures the large-scale variability modes (e.g. ENSO, NAO, and PDO).

In order to predict future weather, teleconnections are important, and the models should be able to capture these to predict correctly. Rajendran et al. (2022) investigated the performance of CMIP6 in the simulation of the climatological Indian summer monsoon rainfall and its teleconnections with interannual modes of variability over the equatorial Pacific and Indian oceans. The results showed that CMIP6 successfully simulated the teleconnection between the Indian summer monsoon rainfall and ENSO in the Boreal summer. However, the model lacks the skill to simulate other important teleconnection patterns. The model also falls short in simulating the teleconnection between the Indian summer monsoon rainfall and Equatorial Indian Ocean Oscillation. In general, the NorCPM captured the dipole structure associated with the Equatorial Indian Ocean



Oscillation but did not capture the link between it and the Indian summer monsoon rainfall.

The model's resolution greatly impacts the degree to which the model can represent complex terrain, which is a dominating feature in Ethiopia. Models with low resolution can experience difficulties representing mountains and the orographic effect that comes with them (Yang et al., 2021). Due to this, the performance of the CMIP6 model will vary with location. According to Yazdandoost et al. (2021), none of the CMIP6 models can represent the orographic precipitation pattern due to the coarse resolution of the model. The same study indicates that the performance of the simulations varies across seasons. An example from the study is that the NorCPM missed the summer rainfall in one region, but in other areas, the summer rainfall was represented well (Yazdandoost et al., 2021).

### 3.3 Statistical Methods

A composite analysis is one way of investigating which factors control the MAM precipitation in Ethiopia. Composite analyses are a simple way to identify conditions observed during a particular climate state. In my thesis these climate states are wet and dry events, meaning years where it rains more (or less) than average. The composites can point out connections between a phenomenon (wet or dry events) and the surroundings and are therefore a tool to capture the relation between precipitation and other variables. However, understanding these relationships requires a combination of different statistical methods and knowledge of the climate system itself (Boschat et al., 2016). By performing a composite analysis one is able to capture asymmetry in different phenomena. In my thesis, I to study anomalies connected to wet and dry events. Thereby, I removed the monthly mean climatology before doing the composite analysis to analyze the anomalies.

The student's t-test was used to check if the composite analysis values were significant. A student's t-test is a way of comparing the means of two groups (Kim, 2015).

In my thesis, the two-sample student's t-test for unequal variance was used, which is given by Equation 3.1. In this equation  $\bar{Y}$  is the mean,  $s$  is the standard deviation, and  $n$  and  $m$  are the sample size. The underscore indicates whether the value is for the first or second population. This equation was used to calculate the t-value. In my case, when doing composites,  $\bar{Y}_1, \bar{Y}_2$  would be the dry and wet composite. In order to see which t-value are significant at the 10% significance level, the degrees of freedom are needed to use the t-table. The degrees of freedom ( $\gamma$ ) for the two-sample student's t-test and unequal variance is given by Equation 3.2 where  $n$  and  $m$  are still the sample size, and  $\sigma$  is the variance (Maity and Sherman, 2006).

$$t = \frac{\bar{Y}_1 - \bar{Y}_2}{\sqrt{(s^2)_1/n_1 + (s^2)_2/n_2}} \quad (3.1)$$

$$\gamma = \left( \frac{(\sigma^2)_1}{n} + \frac{(\sigma^2)_2}{m} \right)^2 * \left( \frac{(\sigma^2)_1/n}{n-1} + \frac{((\sigma^2)_2/m)}{m-1} \right)^{-1} \quad (3.2)$$

Decremer et al. (2014) investigated which significance test performed the best in climate simulations compared to different versions of the bootstrap method. Their results showed that the T-test performed the best in most cases.

An alternative method to analyze relationships between the climate system variables is performing a correlation analysis. An advantage of correlation analysis in comparison to composite analysis is that the correlation is based on all years, while the composites are based on the years under a certain climatic condition. This analysis estimates the linear relationship association between different factors and is a suitable method for investigating the conditions controlling MAM precipitation. Calculating the correlation gives us a coefficient representing the relationship between two variables (Mandyam et al., 2022). The coefficient ( $r$ ) varies between -1 and 1 where values close to 1 or -1 represent high correlation and values close to 0 represent low or zero correlation. The most used correlation coefficient is the Pearson correlation, which is given in Equation 3.3.  $x_i$  represents the values of the x-variable in a sample,  $\bar{x}$  is the mean of the values of the x-variable. The same yields for  $y_i$  and  $\bar{y}$  just for the y variable.

$$r = \frac{\sum_{i=1}^n (x_i - \bar{x})(y_i - \bar{y})}{\sqrt{\sum_{i=1}^n (x_i - \bar{x})^2 (y_i - \bar{y})^2}} \quad (3.3)$$

In my thesis, I used the correlation p-value to check the significance level. The p-value is a probability value describing how likely the results would have occurred by a random chance. The p-value varies between 0 and 1, where values close to zero are classified as significant (McLeod, 2019). In my thesis, I have chosen to look at data where the p-value is smaller than 0.1 (significance level 90%). The exact confidence distribution was used in order to get the p-value. The exact confidence intervals are obtained by solving nonlinear equations and are shown to be very good in the sense that they maintain the coverage percentages for all the parameters at different nominal levels and for different values (Kundu and Ganguly, 2017).

A way of studying spatial patterns of climate variability and how they change over time is to use an Empirical orthogonal function (EOF) analysis. This analysis tool is often used to investigate oscillation systems, which is what I did in this thesis. EOF projects the original climate data on an orthogonal basis. We get this basis by calculating the eigenvectors of a spatially weighted anomaly covariance matrix and a measure of the percent variance explained by each pattern from the corresponding eigenvalues. An EOF analysis can represent mutually orthogonal space patterns where the variance is concentrated. In that way, the first pattern is responsible for the biggest part of the variance, the second for the second largest variance, and so on (Zhang and Moore, 2015). Each EOF is connected to a principal component which provides the sign in addition to the amplitude of the EOF as a function of time (Hannachi, 2004).

# Chapter 4

## Results and Discussion

### 4.1 Selecting study area and timing of the Belg season

Earlier studies done on the Belg season tend to focus on larger regions, like the east Africa region, the Horn of Africa, or the whole of Ethiopia (e.g. Shongwe et al. (2011), Otieno and Anyah (2013), Nicholson (2017) Bekele-Biratu et al. (2018)). This approach is useful for an overview of the Belg season in general and the controlling conditions. In my thesis, I wanted to research the region most affected by the Belg rainfall. The work performed on the Belg season until now partly disagrees with when the Belg season starts. Some papers suggest that the Belg season slowly starts in February and therefore include this month in their calculation, while others only consider March-May.

To select a study area, I calculated the Belg precipitation divided by the annual mean precipitation to estimate where the monthly mean rain in MAM is larger than the climatological monthly mean. Afterward, I masked away all small values, so the remaining area is where the Belg rainfall contributes more than the annual mean. Due to the disagreement regarding when the season starts, I performed this procedure on both the MAM season (Figure 4.1) and FMAM (Figure 4.2). For the MAM divided by the annual mean, I masked away all values smaller than 2, corresponding to a Belg contribution twice as large as the annual mean. For the FMAM season, I masked away all values smaller than 1,5. The reason for using these threshold values was to capture the region in the southeastern part of Ethiopia where the monthly mean rain in MAM is larger than the climatological monthly mean and, simultaneously, avoid the small blue area in northeastern Ethiopia. After masking away these values, I end up with the shaded area in Figure 4.1a and 4.2a. The results show that these two regions are very similar. Looking at the corresponding histograms of monthly rainfall in the identified Belg region in Figure 4.1b and 4.2b, it shows a similarity, which is expected since the area is almost identical. These histograms show the two rainy seasons dominating the southern part of Ethiopia (spring and winter), and February contributes minimally to the spring rainfall. Hence, I will define Belg Season from March to May in this thesis.

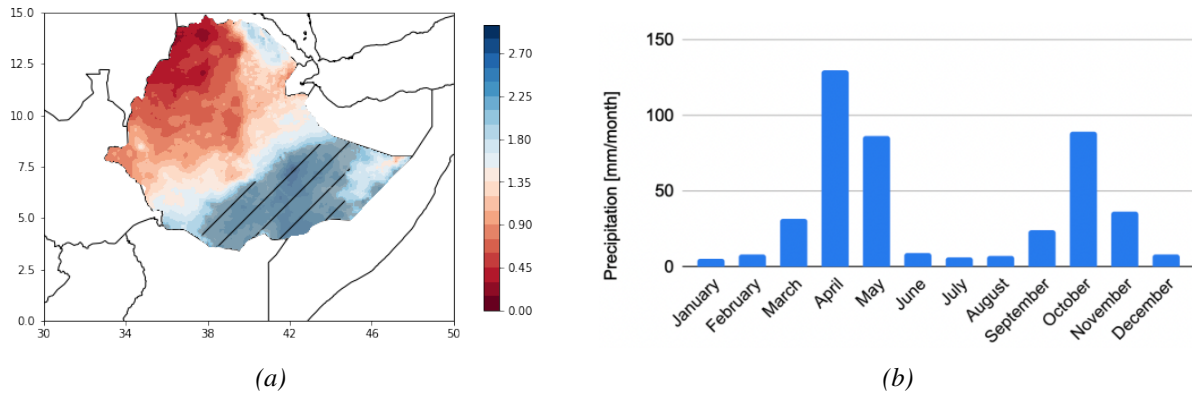


Figure 4.1: Left panel (a) shows an overview of MAM precipitation divided by annual mean over Ethiopia. The blue (red) color indicates where MAM precipitation is larger (less) than the annual mean. The shaded area represents where the values are larger than 2. The right panel shows a histogram with precipitation amount (mm/month) for each month in the shaded area in figure a.

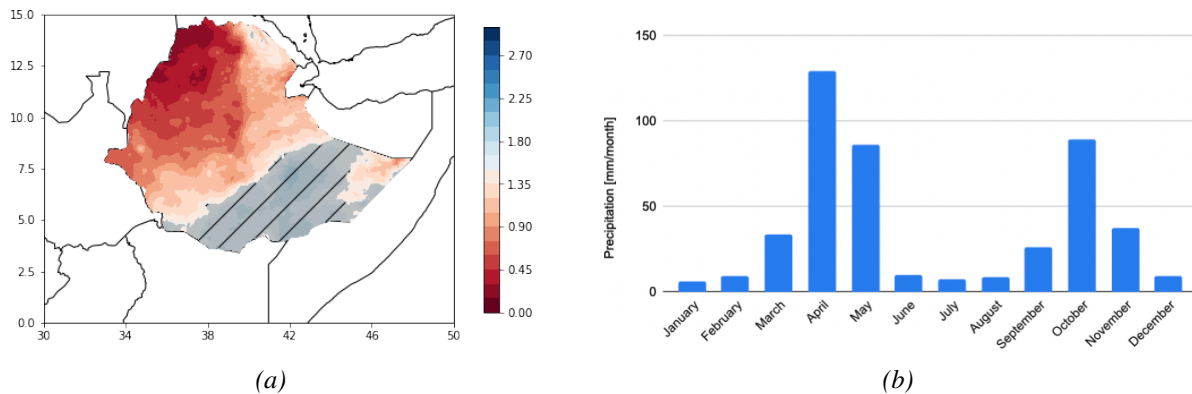


Figure 4.2: Left panel (a) shows an overview of FMAM precipitation divided by annual mean over Ethiopia. The blue (red) color indicates where FMAM precipitation is larger (less) than the annual mean. The shaded area represents where the values are larger than 1.5. The right panel shows a histogram with precipitation amount (mm/month) for each month in the shaded area in figure a.

## 4.2 Choosing the base for composites

To see what factors contribute to the interannual variability of Belg rainfall, I wanted to investigate the years where the MAM precipitation is larger than normal and less than normal in the Belg domain (the shaded area in Figure 4.1a for CHIRPS and A.1 for ERA5). I define these wet and dry years as precipitation exceeding one standard deviation. Figure 4.3 shows a time series of the MAM precipitation in the Belg domain for both CHIRPS (green) and ERA5 (yellow). The straight lines represent the corresponding standard deviation. The reason for doing this procedure to both data sets is to see to which degree the two data sets agree. Observing the time series shows that the time series generally follow each other, but there are some differences in which years are defined as wet and dry. From the aforementioned definition of wet and dry events, the years that were especially wet and dry from the two data sets are shown in Table 4.1 and 4.2.

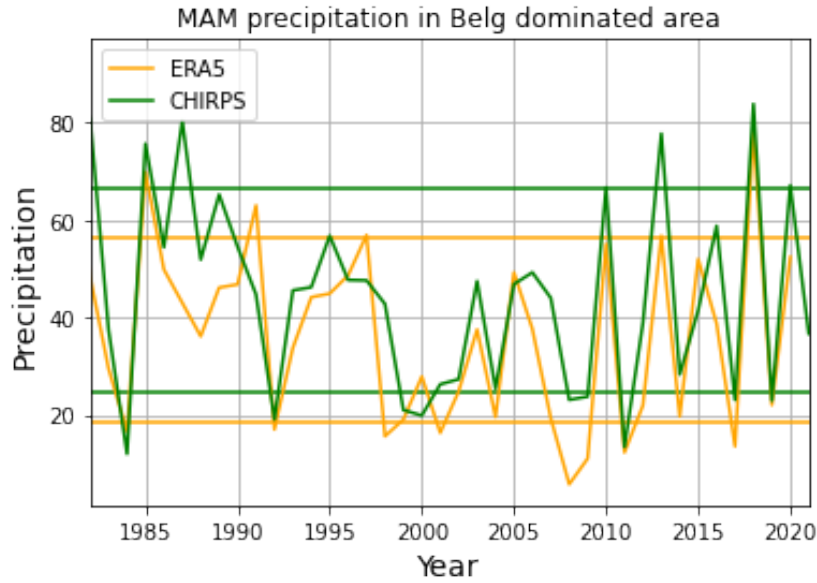


Figure 4.3: A time series of the MAM precipitation [mm/month] in the Belg-dominated area for ERA5 (yellow line) and CHIRPS (green line) from 1981-2021. The corresponding straight line represents the standard deviation.

<b>CHIRPS</b>	1982	1985*	1987	2010	2013*	2018*	2020
<b>ERA5</b>	1985*	1991	1997	2013*	2018*		

Table 4.1: Years with a wet MAM season. Star(\*) indicates wet years in both CHIRPS and ERA5.

<b>CHIRPS</b>	1984*	1992*	1999	2000	2008*	2009*	2011*	2017*	2019	
<b>ERA5</b>	1984*	1992*	1998	2001	2004	2008*	2009*	2011*	2014	2017*

Table 4.2: Years with a dry MAM season. Star(\*) indicates the years that are dry in both CHIRPS and ERA5.

The results in Table 4.1 and 4.2 show that there are some differences in which years that are being defined as wet and dry MAM seasons. Due to the good performance, CHIRPS has shown over Ethiopia in the evaluations (e.g. Dinku et al. (2018)), in addition to that ERA5 struggle with orographic precipitation (e.g. Lavers et al. (2022)), I choose to use the CHIRPS time series as a base in the forward composite analysis. The upper panel years in Table 4.1 and 4.2 were used to make the ongoing composites. I also did composites for the overlapping years (the ones marked with a star in Table 4.1 and 4.2) to see if these differ from choosing the CHIRPS years.

### 4.3 Observation analysis

This section will cover the results using the observations from CHIRPS, NOAA OI SST V2, and ERA5, to see which parameters affect the interannual variability of MAM precipitation in the Belg domain. The main results are based on composite and correlation analysis described in the method section. The motivation for this part is that I wanted to investigate the results from previous studies and see if I could find factors

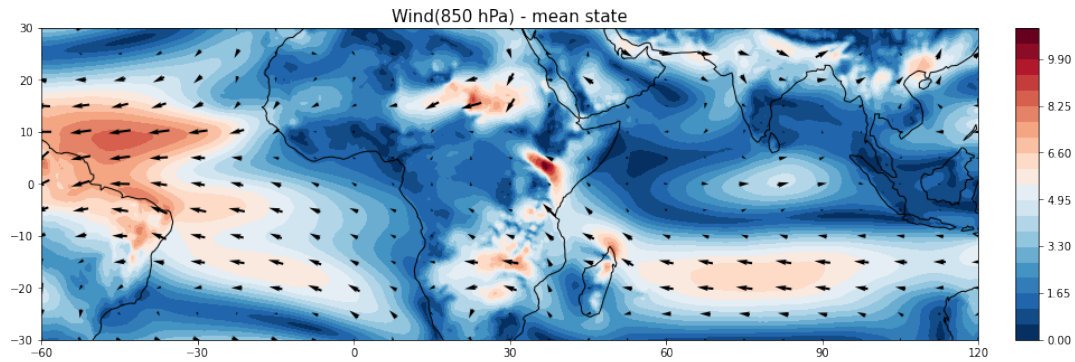


Figure 4.4: MAM mean 850 hPa wind [m/s]. The arrows indicate the wind anomaly's direction and strength, and the contour shading represents the wind strength.

controlling the MAM precipitation in Ethiopia that were not covered in the previous studies on this topic. In addition to this, I wanted to investigate the phenomena in which the research disagrees.

### 4.3.1 850hPa Wind

In order to see what the wind pattern looks like during the MAM season, I plotted the mean 850 hPa winds during MAM. This pattern is shown in Figure 4.4. This result shows that the Somali Jet is visible during the MAM season and might contribute to the amount of moist air towards Ethiopia. The results show that the jet moves towards the west in the southern Indian Ocean and then turns when it reaches the African continent and moves northward towards Ethiopia. Therefore, factors that affect the Somali Jet might also affect MAM precipitation in Ethiopia. This supports the study of Eden et al. (2014).

In this thesis, I also performed a composite analysis on several variables to see what the climate system looks like when there are wet and dry MAM seasons. Figure 4.5 shows a MAM composite for wind (arrows) at 850hPa and specific humidity (contour shading). Black arrows indicate that the wind anomaly is significant at the 10% significance level. The upper panel represents the wet events, while the lower represents the dry events. As expected, for the wet composite shown in figure 4.5a, the specific humidity over Ethiopia and the surrounding area is higher compared to climatology and the opposite for the dry event in figure 4.5b.

The wet MAM years in Figure 4.5a shows easterly winds over the Indian ocean. This pattern is visible over large parts of the Indian Ocean, reaching from the Pacific islands in the east towards Ethiopia in the west. There is reason to believe that these winds bring moist air from the Indian Ocean toward Ethiopia. There are also westerly winds over central Africa, although this signal is weaker than the winds over the Indian Ocean. These winds lead to convergence and positive precipitation anomaly. The dry MAM years in Figure 4.5b shows the opposite pattern with westerlies reaching from the Horn

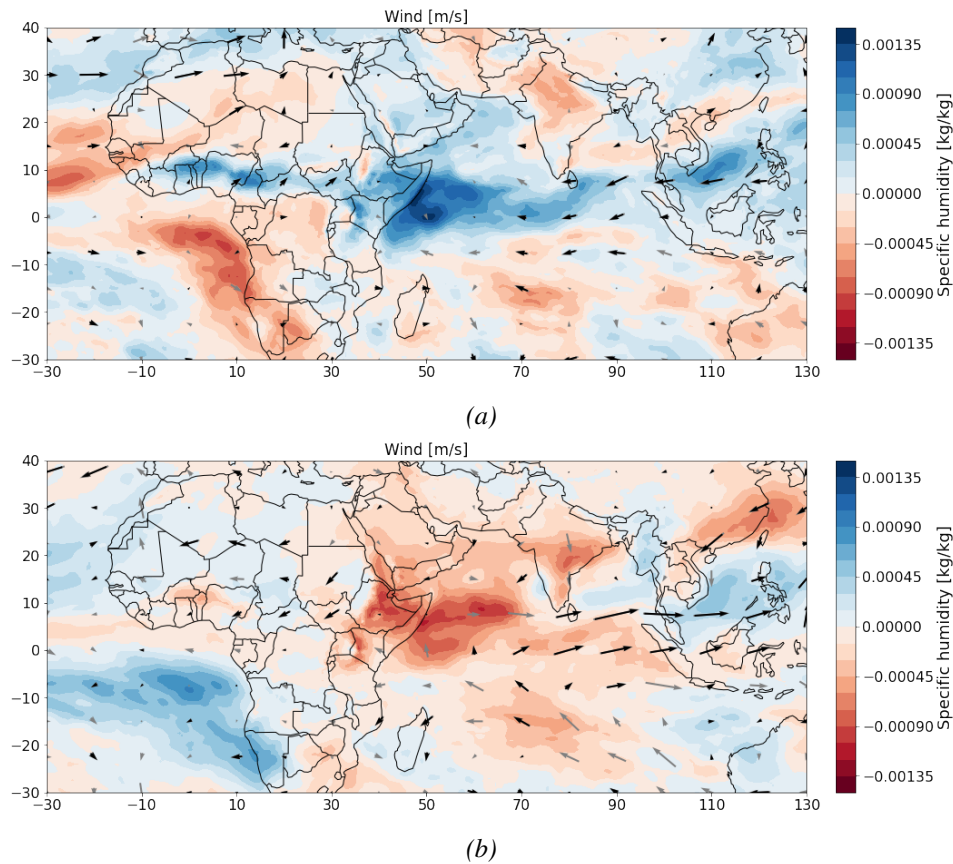


Figure 4.5: MAM wind anomaly [m/s] at 850hPa for wet events (upper figure (a)) and dry events (lower figure (b)). The arrows indicate the wind anomaly's direction and strength. Black arrows indicate values that are significant at the 10% significance level. Grey arrows indicate non-significant values. The contour shading represents specific humidity [kg/kg] anomalies, also at 850hPa height. The blue shading indicates values wetter than climatology, and the red shading indicates drier than climatology.

of Africa towards the Pacific island. The results also show easterly wind anomalies over central Africa, which, combined with the westerlies over the Indian Ocean, will lead to divergence and a dry climate. This pattern is significant at the 10% significance level and indicates a change in the Walker Circulation that takes place over the Indian Ocean. There was also found a significant correlation between MAM precipitation in the Belg domain and 850 hPa winds in the u-direction at the eastern part of the Indian Ocean. This relation is shown in Figure A.2.

### 4.3.2 200hPa Wind

Several studies (e.g. Camberlin and Philippon (2002)) have shown the connection between the Subtropical Westerly Jet (STWJ) and MAM precipitation in Ethiopia. By investigating 200 hPa mean wind during MAM, we get the pattern shown in Figure 4.6, which shows the STWJ as a narrow stream of fast-flowing air between 15°N and 30°N. This suggests that the STWJ is visible during the MAM season.

By performing a composite analysis, I can investigate to which degree the STWJ affects

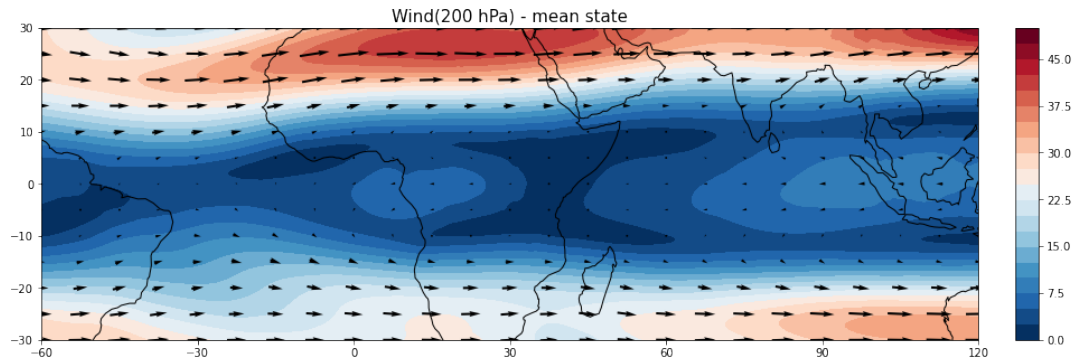


Figure 4.6: MAM mean 200 hPa wind [m/s]. The arrows indicate the wind anomaly's direction and strength, and the contour shading represents the wind strength.

MAM precipitation in the Belg domain. The composites are shown in Figure 4.7. Black arrows indicate that the wind anomaly is significant at the 10% significance level. The wet events shown in Figure 4.7a show a westerly wind anomaly south of the original position of the STWJ. This indicates a southward shift of the Jet. On the other hand, Figure 4.7b represents the 200hPa MAM wind dry composite, which shows the opposite pattern with easterly anomalies over northeastern Africa and a westerly anomaly further north. This suggests a northward shift in the Jet and less precipitation, most likely due to the displacement of the trough. This pattern is significant at the 10% significance level. This connection is also visible in the correlation calculation between MAM precipitation in the Belg domain and 200 hPa wind in the u-direction shown in Figure A.3.

### 4.3.3 SST teleconnections

Figure 4.8 shows the correlation between MAM precipitation in the Belg domain and MAM SST, where four areas stand out. The first area is a small region along the coast of South Africa, Namibia, and Angola. This signal corresponds to the Benguela Niño. The second area to investigate further is the southeast of South Africa, which represents the Agulhas Current. These two areas negatively correlate with MAM precipitation in the Belg domain. The two last areas are located in the northern part of the Pacific Ocean and correspond to a Pacific meridional mode pattern (PMM). The northern patch (PMM-north) has a negative correlation to MAM precipitation in the Belg domain, while the southern patch (PMM-south) has a positive correlation. The same four areas stand out in the composite analysis as well (shown in Figure A.4).

In addition to these four regions, the western Indian Ocean stands out when investigating the correlation between March SST and MAM precipitation in the Belg domain. This signal gets weaker in April and May SST, which makes it not as clear in the SST MAM correlation plot. The correlation between March SST and MAM precipitation over the Indian ocean in addition to the western Indian Ocean area (visualized with a box) I chose to investigate further is shown in Figure 4.9.



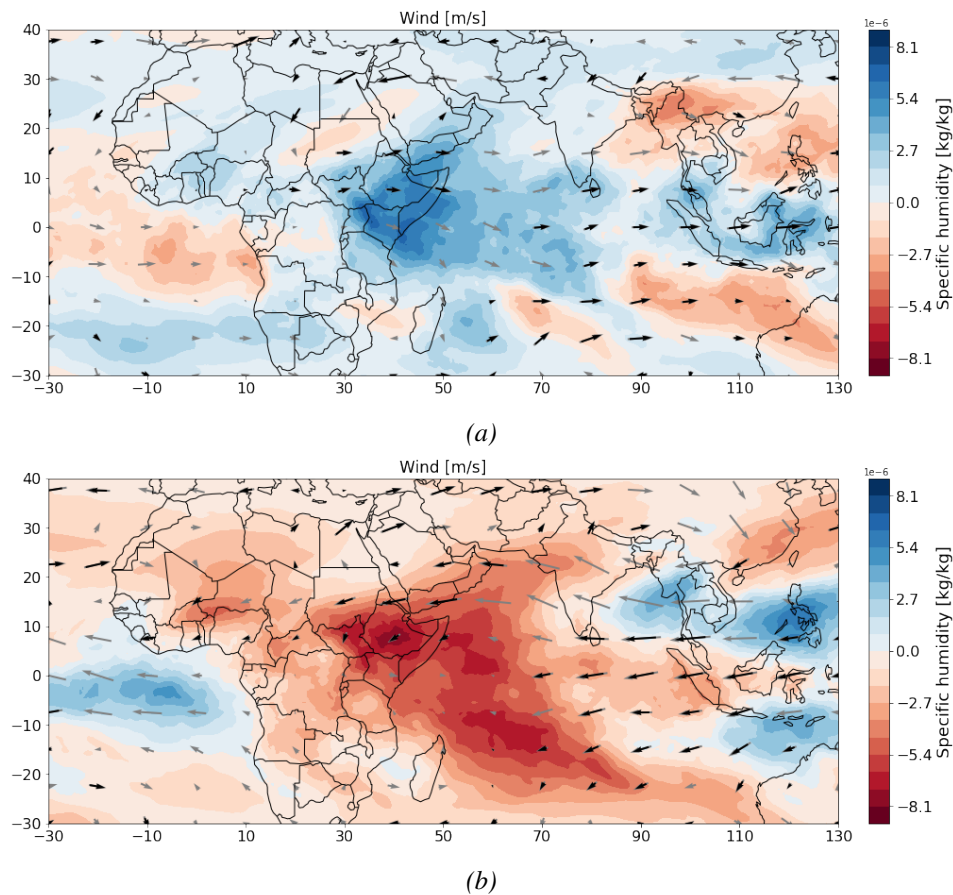


Figure 4.7: MAM wind anomaly [m/s] at 200hPa for wet events (upper figure (a)) and dry events (lower figure (b)). The arrows indicate the wind anomaly's direction and strength. Black arrows indicate values that are significant at the 10% significance level. Grey arrows indicate non-significant values. The contour shading represents specific humidity [kg/kg] anomalies, also at 200hPa height. The blue shading indicates values wetter than climatology, and the red shading indicates drier than climatology.

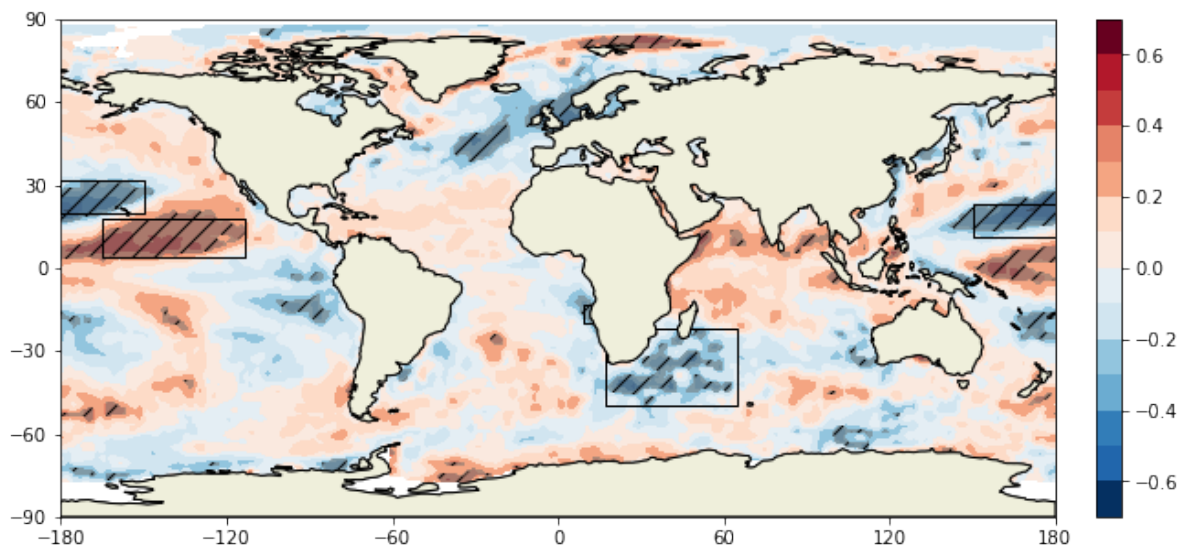


Figure 4.8: Correlation between MAM precipitation in the Belg domain and MAM SST. The red color indicates a positive correlation, while the blue color indicates a negative correlation. The shaded area corresponds to where the correlations are significant at the 10% significance level. The boxes indicate areas with a high correlation that will be investigated further.

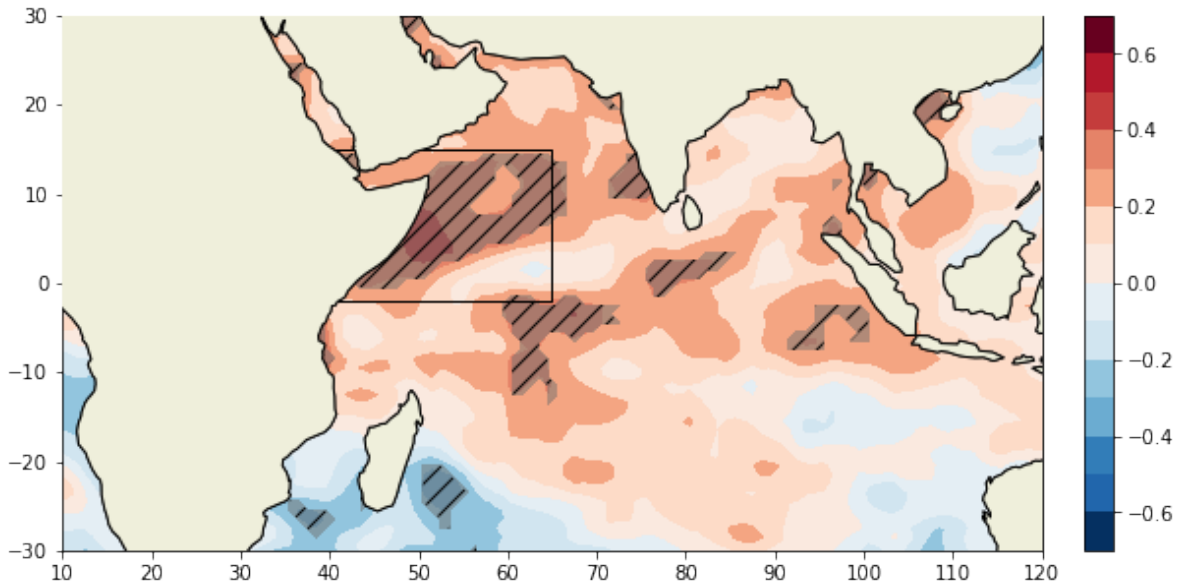


Figure 4.9: Correlation between MAM precipitation in the Belg domain and March SST over the Indian Ocean. The red color indicates a positive correlation, while the blue color indicates a negative correlation. The shaded area corresponds to where the correlations are significant at the 10% significance level. The box indicates the western Indian Ocean area with a high positive correlation that will be investigated further.

These five regions (Agulhas, PMM-North, PMM-South, Benguela, and Indian Ocean) were further investigated to see which month of the SST had the highest correlation with MAM precipitation in the Belg domain. The mean value of SST in the box for each month was correlated with MAM precipitation in Ethiopia. A graph with the correlation between these areas and MAM precipitation in the Belg domain for each month is shown in Figure 4.10. In this Figure, the months indicated with  $t=0$  represent SST in the months the same year as the MAM season are correlated, while months with  $t=-1$  indicates months the year before the MAM season.

Of the five regions, the Benguela Niño and the western Indian Ocean have the overall lowest correlation with MAM precipitation. The only months SST in the Benguela region has a significant correlation to MAM precipitation in Ethiopia are April ( $t=0$ ) and August ( $t=0$ ), with the highest value (-0.31) in August ( $t=0$ ). There was only found a significant correlation between MAM precipitation in the Belg domain and SST in the western Indian Ocean in March and April. The largest correlation was in March ( $t=0$ ) and was 0.32. Due to the low correlation, I choose to focus more on the remaining areas.

The Agulhas region correlates much more with MAM precipitation in the Belg domain than in Benguela and the Indian Ocean. The correlation is significant from September ( $t=-1$ ) and all the way until April ( $t=0$ ) and again in June ( $t=0$ ). The highest correlation is between March SST and MAM precipitation in the Belg domain, with a value of

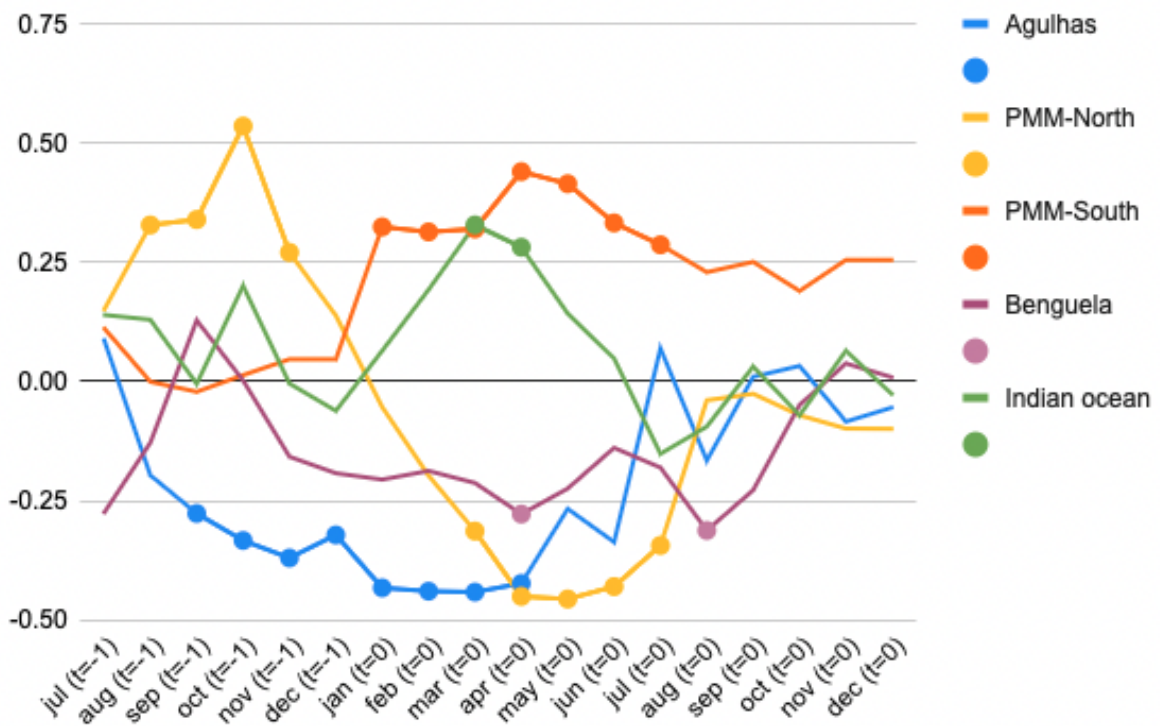


Figure 4.10: Overview of the correlation between MAM precipitation in the Belg domain and SST in the 5 regions Benguela, Agulhas, PMM-north, PMM-south, and the Indian Ocean for each month. The months indicated with  $t=0$  represent SST in the months the same year as the MAM season are correlated, while months with  $t=-1$  indicate that SST the year before the MAM season is correlated. A circle indicates values where the correlations are significant at the 10% significance level.

-0.44. The correlation is negative, meaning that a warm (cold) Agulhas is associated with a dry (wet) Belg season.

But how can the temperature of the Agulhas current affect precipitation in Ethiopia? To investigate this further, I calculated the correlation between MAM SST in the Agulhas region and MAM wind in the v-direction at 850 hPA. This result is shown in Figure 4.11. This figure shows a strong negative signal alongshore Kenya, Tanzania, and Mozambique. This indicates that a warm Agulhas current weakens the Somali jet, affecting Ethiopia's MAM precipitation.

Then the question arises: how does the Agulhas current affect the Somali jet? This can be explained through the Mascarene High. Miyamoto et al. (2022) investigated the maintenance mechanisms of the wintertime Mascarene High. One of the findings in this study was that the Agulhas SST front reinforces the surface Mascarene High. In addition, Chen et al. (2022) found a strong connection between the Mascarene high and the Somali Jet. The study saw that the strength of the Mascarene High affects the Somali Jet and that this connection is strongest during April-May, which matches the timing of the Belg season. Therefore, there is reason to believe that the way the Agulhas current affects MAM precipitation in the Belg domain is through the connection between the Agulhas current and the Mascarene High, which affects the Somali Jet, which thus affects MAM precipitation in Ethiopia. The composites of mean sea level pressure during MAM (Figure 4.12 ) supports this statements since the Mascarene High is strong in the dry composite, and weak in the wet composite. This composite is not significant, most likely due to the high variability of mean sea level pressure.

In addition to the Agulhas current, both PMM signals also show some significant correlations. The southern patch has a significant positive correlation in the entire period from January-July. The northern patch gives a more surprising pattern. The results show a change in sign of the correlation when looking at the months the year before ( $t=-1$ ) compared to the same year ( $t=0$ ). The correlation is positive and significant from August ( $t=-1$ ) to November ( $t=-1$ ) and negative and significant from March ( $t=0$ ) until July ( $t=0$ ). The correlation is quite large on both sides, with the highest positive correlation being 0.535 and taking place in October ( $t=-1$ ) and the highest negative correlation being -0.45 and taking place in May. The correlation is overall quite high, but the large jump between October ( $t=-1$ ) and March ( $t=0$ ) is quite surprising.

In order to investigate how the PMM pattern can affect MAM precipitation in the Belg domain, I calculated the correlation between MAM SST in the northern and southern PMM patches and 850 hPA winds in the U-direction the same months to see if there is a connection here. These results are shown in Figure 4.13. Figure 4.13a shows the correlation between MAM SST in the northern PMM patch and MAM wind in the

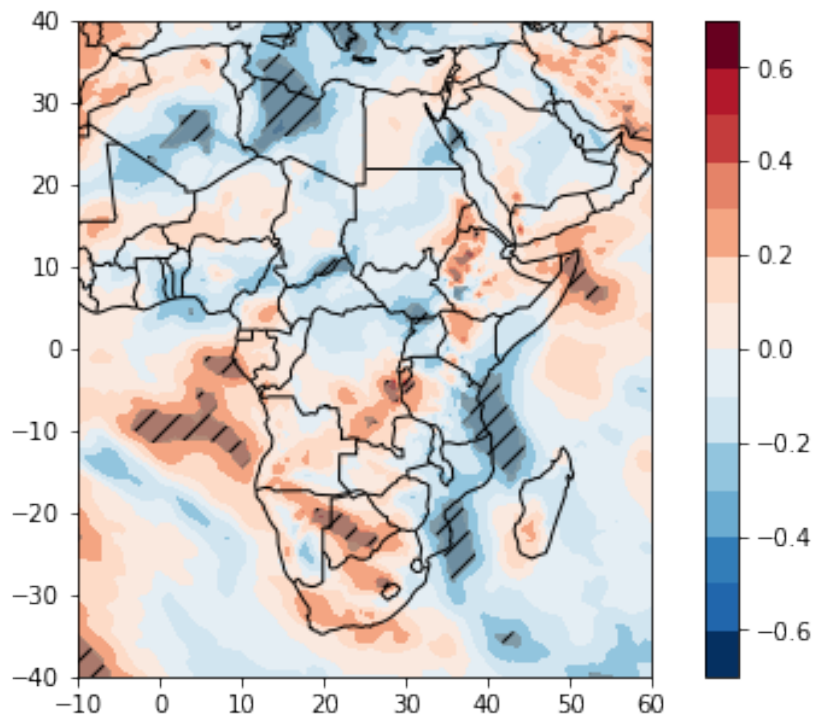


Figure 4.11: Correlation between MAM SST in the Agulhas region and MAM wind in V-direction at 850 hPa. The red color indicates a positive correlation, while the blue color indicates a negative correlation. The shaded area corresponds to where the correlations are significant at the 10% significance level.

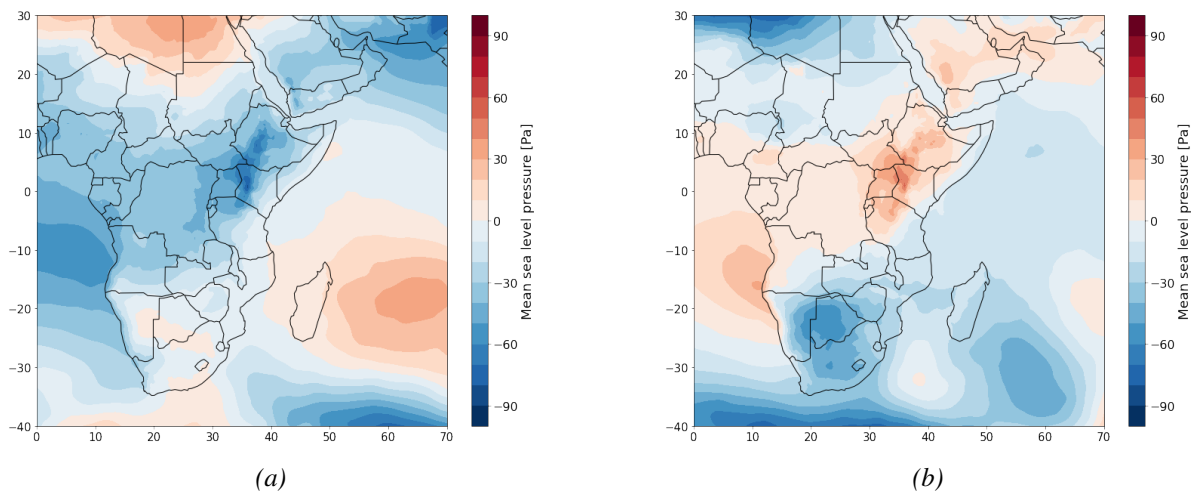


Figure 4.12: MAM mean sea level pressure anomaly [Pa] at for dry events (figure a) and wet events (figure b). The blue shading indicates negative pressure anomaly, and the red shading indicates positive pressure anomaly.

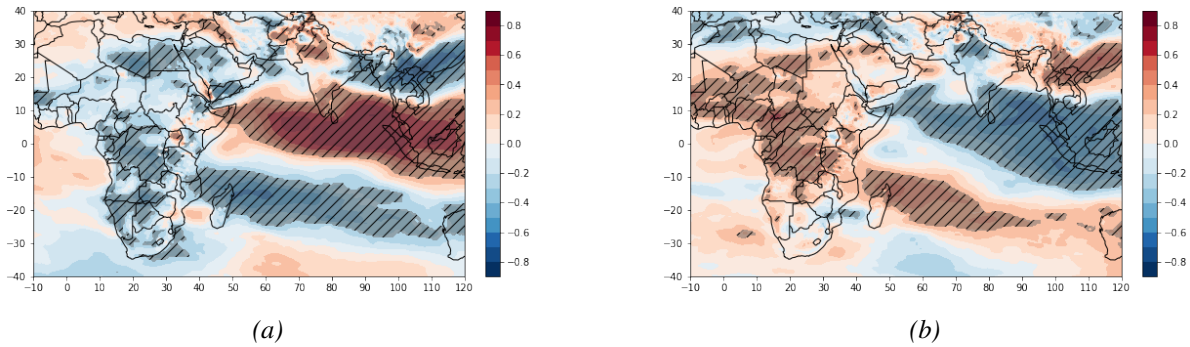


Figure 4.13: Left panel: Correlation between MAM SST in the northern PMM patch and MAM wind in U-direction at 850 hPa. Right panel: same as the left one but for the southern PMM patch. The red color indicates a positive correlation, while the blue color indicates a negative correlation. The shaded area corresponds to where the correlations are significant at the 10% significance level.

U-direction. There is a strong positive correlation in the northern Indian Ocean and a strong negative correlation in the southern Indian Ocean. The positive correlation in the north is interesting here since it reaches all the way from Ethiopia in the west and towards the Pacific Islands. This suggests that when the northern PMM patch is warm (cold), the winds over the northern Indian Ocean towards Ethiopia weaken (enhance), and less (more) moist air will advect towards the Belg domain. This result matches my expectations since I know from Figure 4.8 that the northern patch of the MAM PMM is negatively correlated with MAM precipitation in the Belg domain.

On the other hand, Figure 4.13b (same as 4.13a, just for the southern PMM patch) shows an opposite pattern. There is a strong negative correlation in the northern Indian Ocean and a strong positive correlation in the southern Indian Ocean. Looking further into the negative correlation in the North Indian Ocean, which also stretches from Ethiopia toward the Pacific Islands. This indicates that a warm (cold) southern PMM patch enhances (weakens) the winds over the northern Indian Ocean towards Ethiopia and increases (decreases) the amount of moist air advecting towards Ethiopia. This also matches my expectations since I can see from Figure 4.8 that the southern patch of the PMM is positively correlated with MAM precipitation in the Belg domain.

So, how is the PMM pattern connected to winds in the northern Indian Ocean? Hari et al. (2022) investigated the connection between north Pacific variability and Indian summer heatwaves. In this study, they saw that the PMM pattern weakens the zonal Walker circulation over the Pacific, changing the lower-level westerlies into easterlies over the Indian Ocean. This matches the results and suggests that the PMM pattern affects the Ethiopian rainfall by affecting the Walker circulation.

#### 4.3.4 ENSO

As mentioned in the Method section, there is disagreement on which degree the ENSO affects the MAM season in Ethiopia. There is a small ENSO signal showing in the

correlation plot (Figure 4.8) and SST composite (A.4), but it is weaker than the other areas. To investigate this relationship further, I performed a composite analysis based on warm and cold ENSO events. By selecting the Niño 3.4 area and looking at the SST time series for DJF in this region, I could see which years had a warm and cold ENSO by using the same definition as earlier: when the value exceeds the standard deviation. The warm years turned out to be: 1983, 1987(wet year), 1992(dry year), 1998, 2015, and 2016. On the other hand, the cold years were: 1984(dry year), 1985(wet year), 1989, 1999(dry year), 2000(dry year), 2008(dry year), and 2011(dry year). The parenthesis indicates if the year was dry or wet in the Belg domain using CHIRPS data (Table 4.1 and 4.2).

The precipitation pattern over Ethiopia in MAM during a warm and cold ENSO is shown in Figure 4.14. Figure 4.14a illustrates the precipitation pattern in MAM during a La Niña (cold ENSO). For the Belg domain in the southeastern part of Ethiopia, La Niña affects the precipitation here as a negative precipitation anomaly takes place in this region. This anomaly varies between -5 and -45 mm/month. Figure 4.14b shows the precipitation pattern during an El Niño event (warm ENSO). By looking at the Belg domain in the southeastern part of Ethiopia, it shows that the pattern is less clear. The signal is much weaker compared to the La Niña scenario. In addition to that, the signal is both positive and negative in the area of interest in this thesis. The result shows that there are negative precipitation anomalies in southwestern Ethiopia while positive in the southeastern part. These results show that a La Niña event might affect the precipitation in the Belg domain, while an El Niño event is more uncertain to the degree it affects MAM precipitation in Ethiopia. However, this relationship is not significant at the 10% significance level.

This relation was also explained by Anderson et al. (2023), who investigated how multiyear La Niña events led to drought in the Horn of Africa. The study's results showed that the warm SST anomaly in the western Pacific associated with a La Niña event leads to an enhanced Walker circulation and larger subsidence and drought over the Horn of Africa. The study saw this effect both on the MAM season and the OND season. La Niña events are quite predictable. Therefore, better predictability of La Niña events and understanding of its impacts on the horn of Africa can be useful in predicting MAM rainfall in Ethiopia.

### 4.3.5 NAO

As mentioned in the method section, the connection between MAM precipitation in Ethiopia and NAO has been investigated in the past. To investigate this, I looked at composites for geopotential height at 850hPa to see if I could find a connection here. This composite can be seen in Figure 4.15. The wet composite (Figure 4.15a) shows a positive anomaly over Iceland and a negative anomaly over the Azores. This indicates a negative NAO index. For the dry composite (Figure 4.15b) the signal is weaker, but an opposite pattern with a negative anomaly exists over Iceland and a weak positive

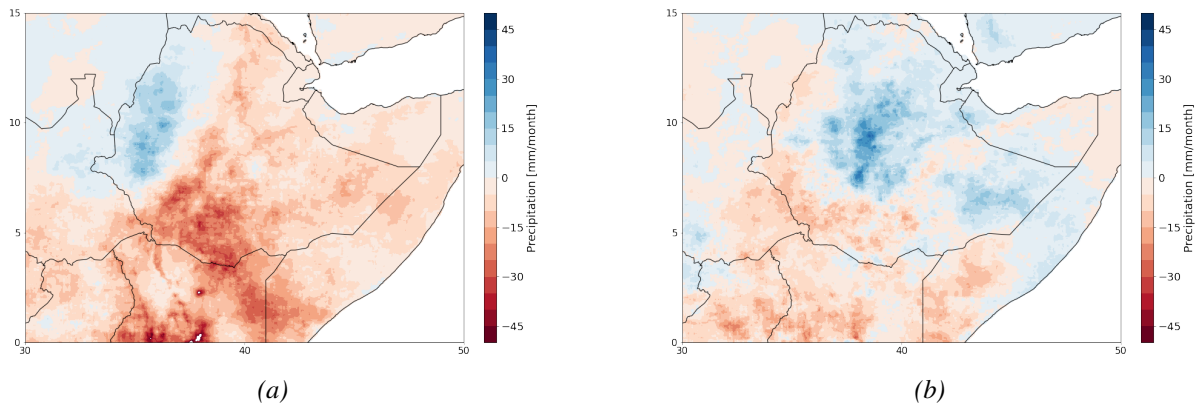


Figure 4.14: MAM precipitation [mm/month] anomaly over Ethiopia for cold ENSO events (left figure(a)) and warm ENSO events (right figure (b)). The blue shading indicates more precipitation than climatology, and the red shading indicates less precipitation than climatology.

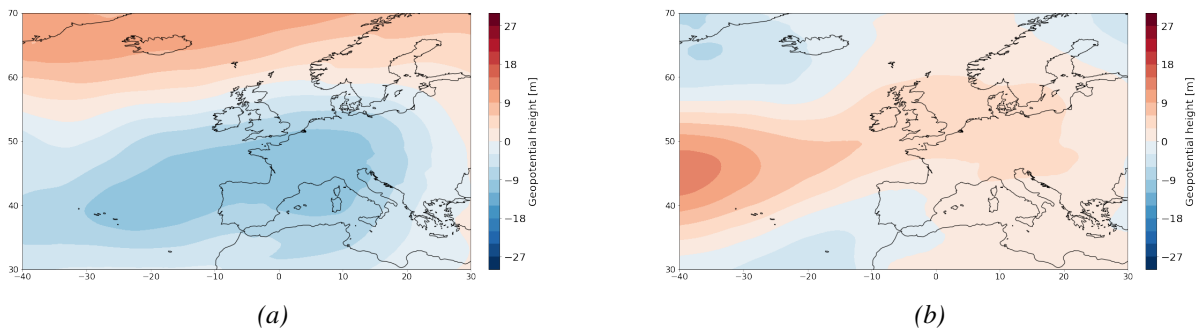


Figure 4.15: MAM geopotential height [m] (850hPa) anomaly for wet events (left figure(a)) and dry events (right figure (b)). The red shading indicates a larger geopotential height than climatology, and the blue shading indicates a lower geopotential height than climatology.

anomaly over the Azores. In contrast to the wet composite, this indicates a positive NAO index. This result matches the study by Williams and Kniveton (2011). While the composite show that there might be a relation between MAM precipitation in Ethiopia and NAO, the correlation plot (not shown) does not show any significant relation.

To investigate this relationship further I used mean sea level pressure (JFMA) to calculate the first EOF and the corresponding principal component. These are shown in Figure 4.16. The first EOF in Figure 4.16a shows this NAO signal with negative anomaly over Iceland and positive over the Azores. The correlation between the first principal component in Figure 4.16b and the time series of precipitation in the Belg domain (4.3) is -0.22 and not significant (p-value > 0.1). This suggests that the NAO is not a contributor to rainfall variability in Ethiopia during MAM season.

However, even though there is no direct correlation between the NAO index and MAM precipitation in the Belg domain, one can not rule out a connection. To investigate this relation further, I performed a composite analysis here to see if I could see a pattern here. The aim was to examine the MAM precipitation pattern years when the



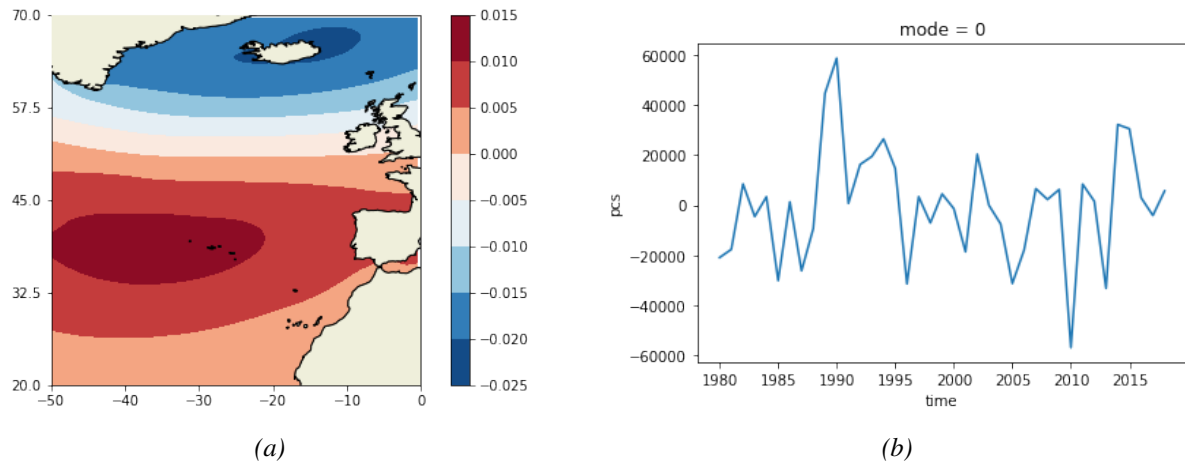


Figure 4.16: Left panel represents the first EOF of the mean sea level pressure over the Atlantic Ocean. The color bar represents explained variability by the first EOF. The figure to the right represents the corresponding principal component.

NAO index was positive and negative. Using the PC1 shown in Figure 4.16b and the aforementioned method of selecting year by using the standard deviation, the years with positive and negative NAO can be found. There are positive NAO indexes in 1989, 1990, 1994, 2014, and 2015, and a negative NAO index in 1985(wet), 1987(wet), 1996, 2005, 2010(wet), and 2013(wet). The parenthesis indicates if the year was dry or wet in the Belg domain using CHIRPS data (Table 4.1 and 4.2).

These composites are shown in Figure 4.17a for negative NAO and 4.17b for positive NAO. In the case of negative NAO, the results show a positive precipitation anomaly over most parts of Ethiopia, but the largest anomaly takes place over the central parts of the country. This indicates that a negative NAO leads to enhanced precipitation in Ethiopia during MAM, which matches with the previously done research and our geopotential height composite shown in Figure 4.15. However, on the composite with a positive NAO index, one can not observe a clear precipitation pattern over Ethiopia during MAM. The precipitation anomalies are weak and switch between being positive and negative in the Belg domain. These results show that a positive NAO index does not significantly impact the MAM precipitation in the Belg domain. However, a negative NAO index seems to lead to enhanced precipitation in entire Ethiopia during MAM. However, by using the student's t-test, this relationship is not significant.

## 4.4 NorCPM

In my thesis, I wanted to evaluate two CMIP6 models against each other and compare them to the results from the observational data. For this purpose, the same method was used.

Starting with the NorCPM model, the (ensemble mean) MAM precipitation divided by (the ensemble mean) annual mean precipitation is shown in Figure 4.18. This result shows a very different pattern compared to using CHIRPS (shown in Figure 4.1). In

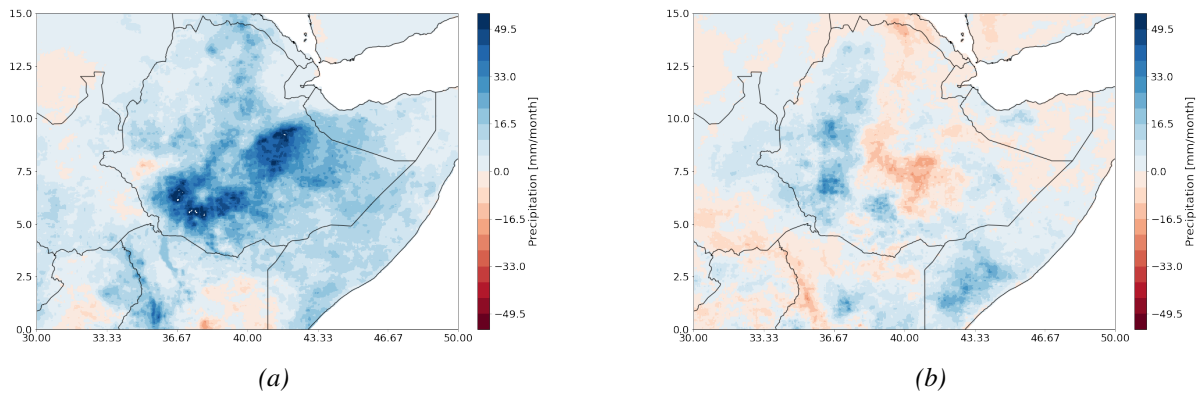


Figure 4.17: MAM precipitation[mm/month] anomaly over Ethiopia for years with negative NAO index (left figure(a)) and positive NAO index(right figure (b)). The blue shading indicates more precipitation than climatology, and the red shading indicates less precipitation than climatology.

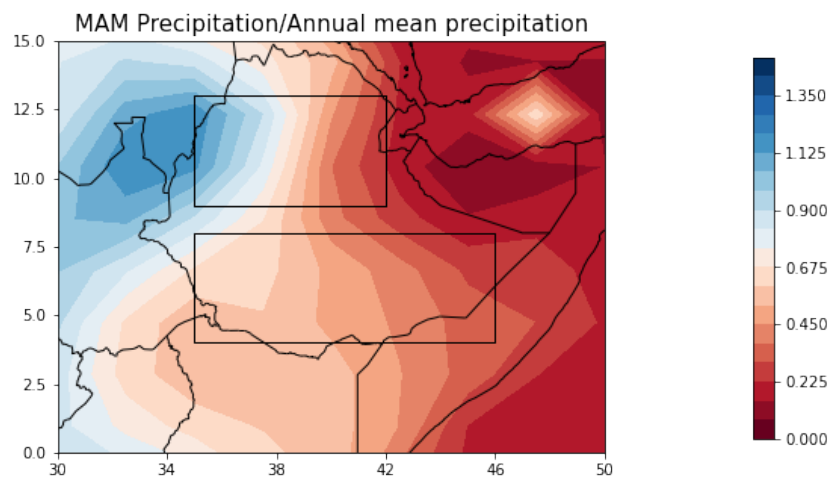


Figure 4.18: An overview of MAM precipitation divided by annual mean over Ethiopia from the NorCPM. The ensemble mean from all 30 ensemble members was used in this calculation. The blue (red) color indicates where MAM precipitation is larger (less) than the annual mean.

the CHIRPS calculation, the MAM precipitation dominated in the southeastern part of Ethiopia (which agrees with previous studies on this topic). The NorCPM calculation in Figure 4.18 shows the highest values in the northwestern part of Ethiopia, which is in the opposite part of Ethiopia compared to the CHIRPS calculation. The Background section showed that this area is more dominated by summer rainfall than spring rainfall.

To investigate this further and see to which degree NorCPM can resemble MAM precipitation in Ethiopia, I chose two boxes, one in North Ethiopia and one in South Ethiopia (also shown in Figure 4.18). I made two corresponding histograms showing precipitation each month in these regions. These histograms are shown in Figure 4.19a for the northern box and 4.19b for the southern box. The histograms are also based on the ensemble mean of the 30 available ensemble members. In the northern box, the model reproduces the summer(JJA) quite well. There is also a large peak in September which is not included in the summer or autumn rainfall. In southern Ethiopia, there is a small peak in June and one larger in October. The MAM season is not as visible in the

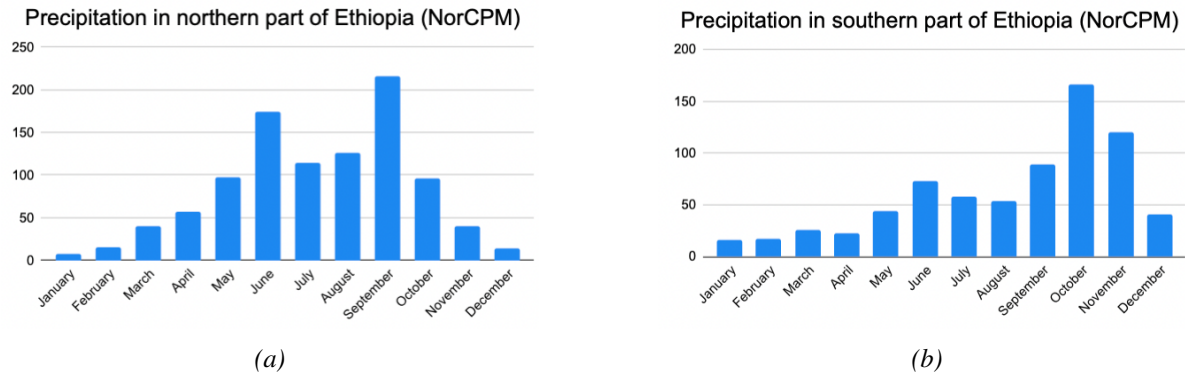


Figure 4.19: Histogram with precipitation[mm/month] amount for each month in northern and southern Ethiopia in the boxes selected in Figure 4.18. The left panel shows a histogram for the northern box, and the right panel shows the southern box. The histograms are based on the ensemble mean of the 30 available ensemble members.

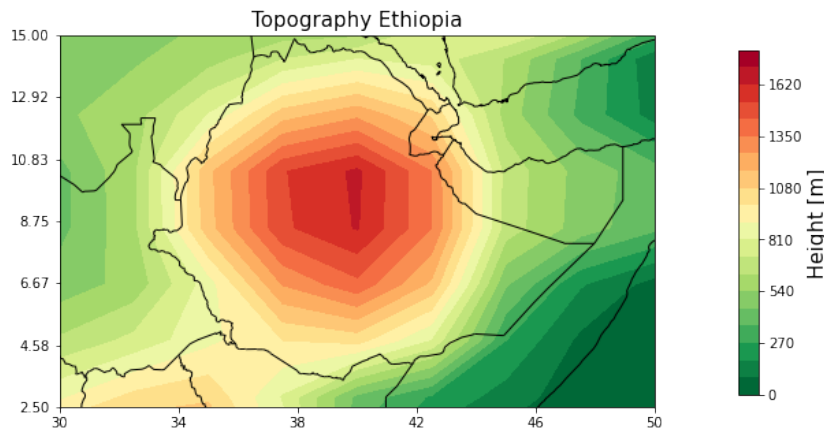


Figure 4.20: Topography[m] distribution used in NorCPM in Ethiopia. Green color represents lowlands while orange represents highlands.

histogram as in the CHIRPS calculation in Figure 4.1b. Thereby, the NorCPM cannot resemble the MAM precipitation in South Ethiopia. The values are also higher for both histograms compared to the CHIRPS histogram shown in Figure 4.1b.

The topography used in the NorCPM is shown in Figure 4.20. Compared to the real topography in Figure 2.1, the topography for the model is affected by the low resolution. In addition, the highlands' location is shifted to the east, and the pattern is more circular compared to oval-shaped as the topography actually is. The magnitude is also much smaller compared to the real world.

## 4.5 NorESM2-MM

Using the same method for the NorESM2-MM as I did on the CHIRPS data and the NorCPM, the MAM precipitation divided by the annual mean as shown in Figure 4.21. The upper panel utilizes all the available years (1850-2014), and the bottom panel shows the same figure for the years available in the CHIRPS data (1981-2014). Firstly,

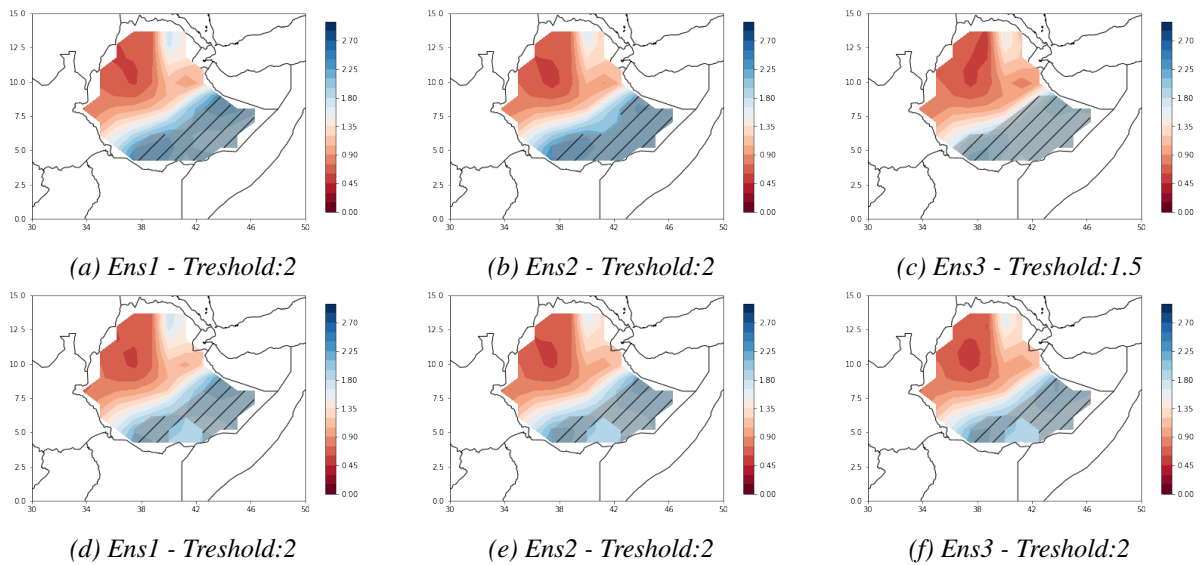


Figure 4.21: An overview of MAM precipitation divided by annual mean over Ethiopia from the NorESM2-MM for two periods and individually for each ensemble member. The shaded area illustrates where the MAM precipitation is significantly larger than the annual mean, so when the MAM/annual means is larger than the threshold value under each figure. The upper panel shows the calculation for 1981-2014, while the bottom panel shows the calculation for the entire available time period (1850-2014). The figures to the left are for ensemble member 1, the central represents ensemble member 2, and the right figures are for ensemble member 3. The blue (red) color indicates where MAM precipitation is larger(less) than the annual mean.

the figures show that they are very similar to the MAM precipitation divided by annual mean precipitation for CHIRPS (shown in Figure 4.1). The background for doing this with both periods and every individual ensemble member is to see if there are large differences between periods and ensemble members in the model data. There are small differences between the two time periods. Due to this similarity, I choose to use the entire time period further to get as much data as possible. The results from Figure 4.21 also show that there are small differences between the different ensemble members. Therefore it is reasonable to use an ensemble mean for the entire period when selecting the Belg domain. This is shown in Figure 4.22.

In addition to this, I wanted to see if all three ensemble members could reproduce the two rainy seasons in South Ethiopia. I created a histogram with the monthly precipitation inside the shaded area in Figure 4.22 to accomplish this. This histogram is shown in Figure 4.23. This figure shows that all of the ensemble members can capture both rainy seasons in this region. There are also very small differences between the ensemble members, especially in the spring. Ensemble member 3 underestimate the precipitation amount in November, but in general, the ensemble members are quite similar.

To investigate the annual variation between the ensemble members and make the base for composite analysis, I made a time series of MAM precipitation in the shaded area

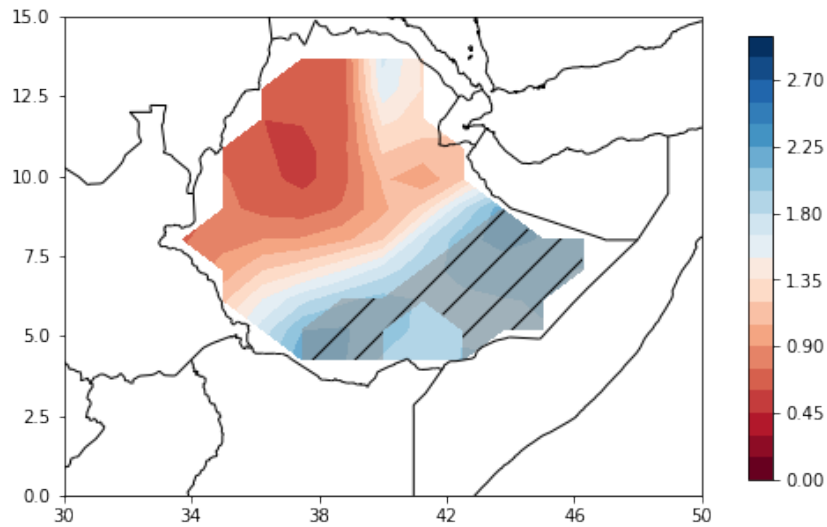


Figure 4.22: The figure shows an overview of NorESM2-MM MAM precipitation divided by annual mean over Ethiopia. The calculation used the ensemble mean of all three ensemble members from 1850 to 2014. The blue (red) color indicates where MAM precipitation is larger (less) than the annual mean. The shaded area represents where the values are larger than 1.9.

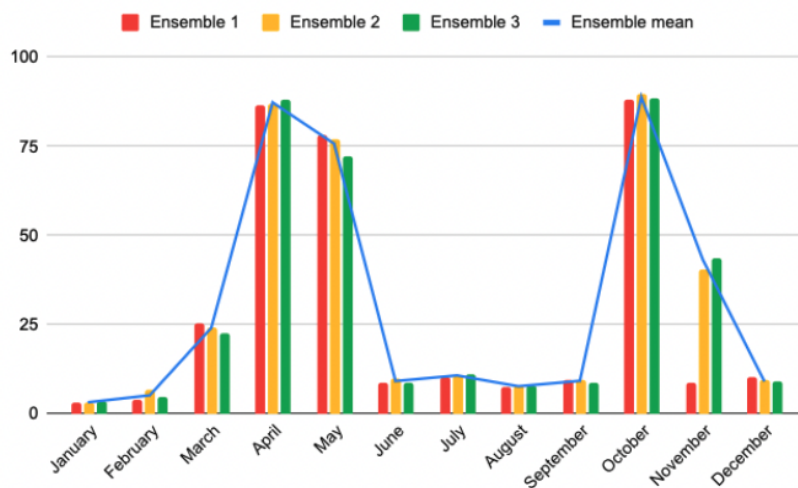


Figure 4.23: histogram with precipitation[mm/month] amount for each month and every ensemble member in the shaded area in Figure 4.22. The red bar shows the result for ensemble member 1, yellow for ensemble member 2, and green for ensemble member 3. The blue line represents the ensemble mean of the three members.

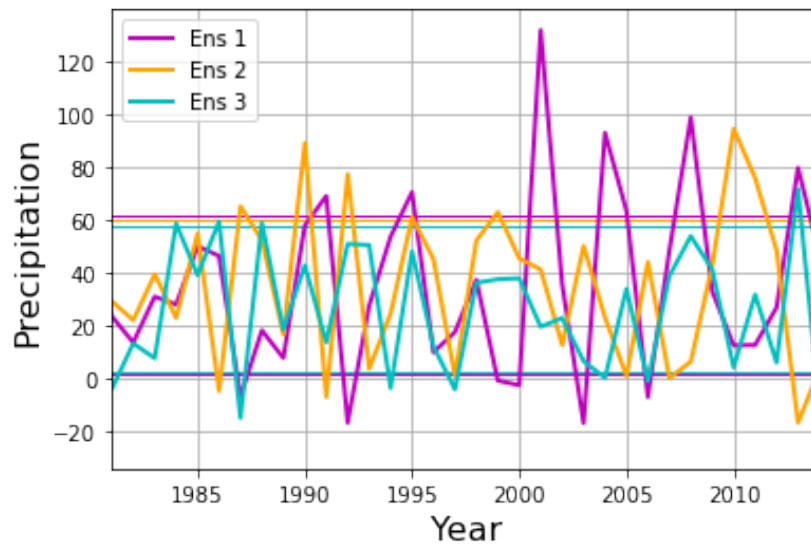


Figure 4.24: A time series of the MAM precipitation [mm/month] in the Belg-dominated area (shaded area in Figure 4.22) for ensemble member 1 (magenta), ensemble member 2 (yellow) and ensemble member 3 (blue) from 1981-2014. The corresponding straight lines represent the standard deviation.

in Figure 4.22 of the three ensemble members. The time-series were made for the years available for the CHIRPS data (1981-2014), so I could compare them. This time series is shown in Figure 4.24. This figure shows that the wet and dry years in the different ensemble members are quite different. There are no years that are wet/dry for all three ensemble members, as expected in coupled climate models. However, there is a similarity in the number of wet or dry years. All three ensemble members have 6 dry years. When it comes to the wet years, there are eight wet years in ensemble member 1, six in ensemble member 2, and three in ensemble member 3. Since the ensemble members have different wet and dry years, the years used in the composite analysis will be different for the different members.

The analysis done on NorESM2-MM and NorCPM shows that NorESM2-MM is more capable of resembling the MAM precipitation in Ethiopia than the NorCPM. One reason for the better representation in NorESM2-MM is the topography used. The Background section showed that the topography is important when visualizing the precipitation pattern. Looking at the topography used in NorESM2-MM in Figure 4.25 shows that the highlands are more oval-shaped and more correctly placed compared to reality (shown in Figure 2.1). This topography is more similar to reality, which might be one reason the NorESM2-MM represents the MAM precipitation in Ethiopia better than the NorCPM. In addition to this, NorESM2-MM has a higher resolution compared to NorCPM. However, there might be other just as important factors affecting this. Due to the better representation of MAM precipitation in the NorCPM, I choose to use this model in further analysis.

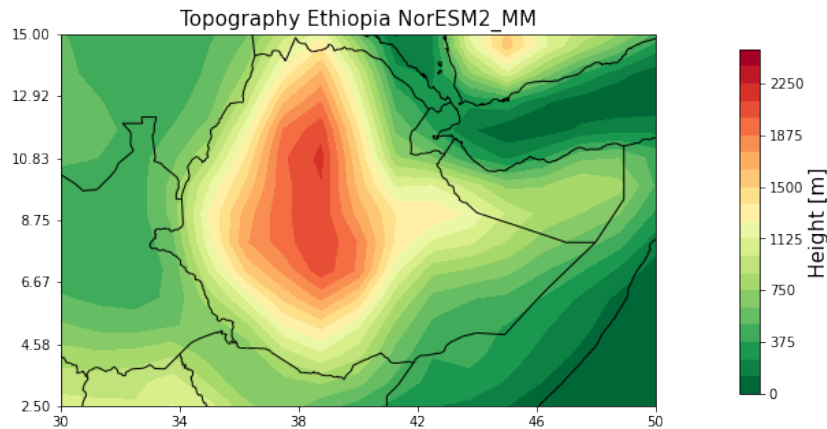


Figure 4.25: Topography[m] distribution used in NorESM2-MM in Ethiopia. Green color represents lowlands while orange represents highlands.

## 4.6 NorESM2-MM - analysis

For the NorESM2-MM model to predict precipitation in Ethiopia, it should be able to capture the factors that affect the MAM precipitation in Ethiopia. In order to check this, I wanted to do the same analysis with the model as I did with the observations in the previous section of this thesis. The next section will cover this analysis with composites and correlation plots that will be used in comparison with the observations. The composites are based on the same period as CHIRPS was available (1981-2014), and the entire time period was used for the correlation calculations.

### 4.6.1 Wind 850 hPa - NorESM2-MM

The observations showed that westerlies in the Indian Ocean led to a dry Belg season and that easterlies in the Indian Ocean led to a wet Belg season. To compare the NorESM2-MM to the observation, I performed a composite analysis of 850hPa winds from the model. These results are shown in Figure 4.26. The dry events in the right panels show that all ensemble members show a negative specific humidity anomaly over Ethiopia, as expected for the dry event case. However, ensemble members 1 and 2 show easterly winds over the Indian Ocean, which is the opposite of the observation composite showed. Physically, this is a bit unexpected since it suggests moist air from the Indian Ocean to advect towards Ethiopia. These two composites also show a westerly component over the African continent, although the observations suggested weaker winds over the African continent. In the dry event for ensemble member 3, it is a negative specific humidity anomaly, in addition to a more mixed pattern over the Indian Ocean with both weak westerlies and easterlies. The three ensemble members in the wet scenarios show that all ensemble members are able to reproduce the positive specific humidity anomaly over Ethiopia. The results show westerly winds over the Indian Ocean, which is the opposite of the results in the observations. The three ensemble members show a westerly flow from the Atlantic Ocean all the way toward Ethiopia. These results show that the NorESM2-MM output suggests that the moisture during wet events comes from the Atlantic and not the Indian Ocean which

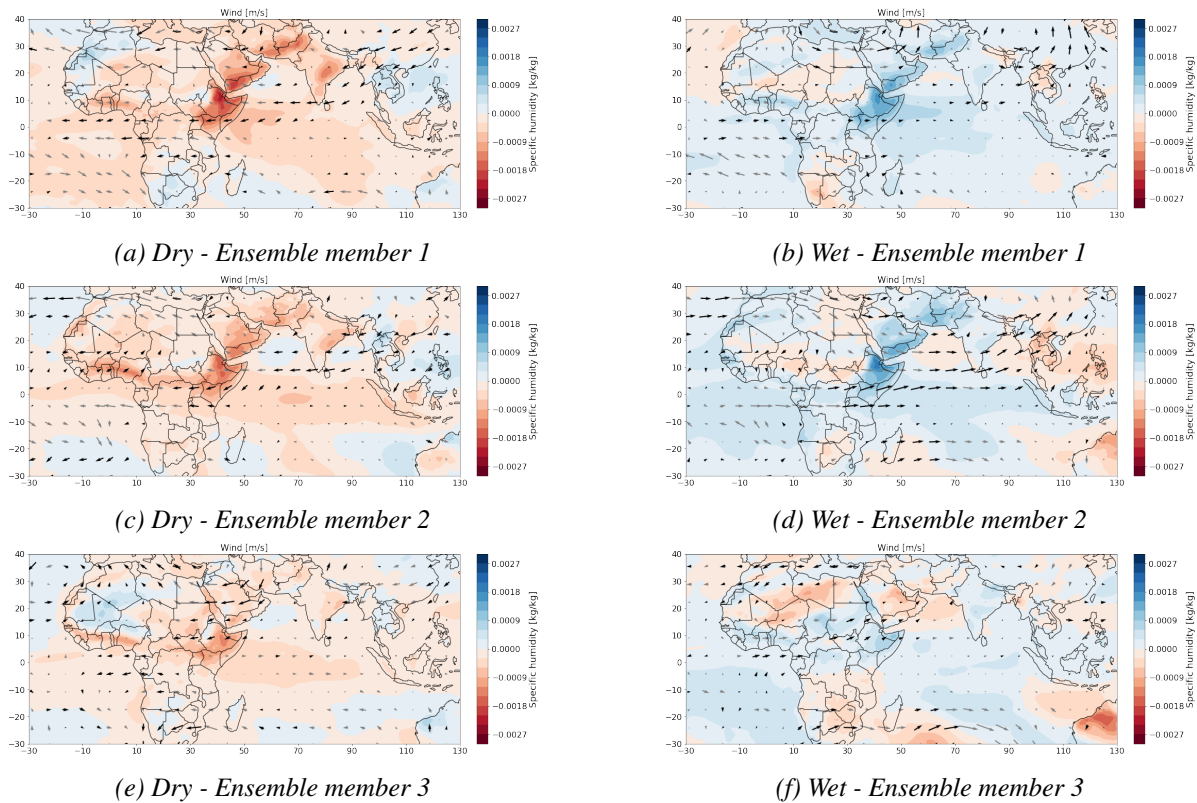


Figure 4.26: MAM wind [m/s] (850hPa) anomaly from three ensemble members of the NorESM2-MM. Dry events are shown to the left, and wet events are shown to the right. The arrows indicate the wind anomaly direction and strength. Black arrows indicate values that are significant at the 10% significance level. Grey arrows indicate non-significant values. The contour shading represents specific humidity [kg/kg] anomalies, also at 850hPa height. The blue shading indicates values wetter than climatology, and the red shading indicates drier than climatology.

the observations suggested.

## 4.6.2 Wind 200 hPa - NorESM2-MM

The composite analysis for NorESM2-MM winds at 200hPa is shown in Figure 4.27. None of the ensemble members are able to capture the displacement of the STWJ during wet and dry years. In the observation we saw for the dry years, we saw easterly anomalies over northeastern Africa and a westerly anomaly further north. The left panel in Figure 4.27 shows that ensemble member 1 is partly able to recreate this pattern with the easterly anomaly over the northeast of Africa, but it is not able to capture the westerly anomaly further north. Ensemble members 2 and 3 are not able to capture any of these patterns. The observations showed for the wet events a southward shift in the STWJ, which was represented by a westerly wind anomaly south of the original position of the STWJ. None of the ensemble members in the right panel of Figure 4.27 are able to recreate this pattern.



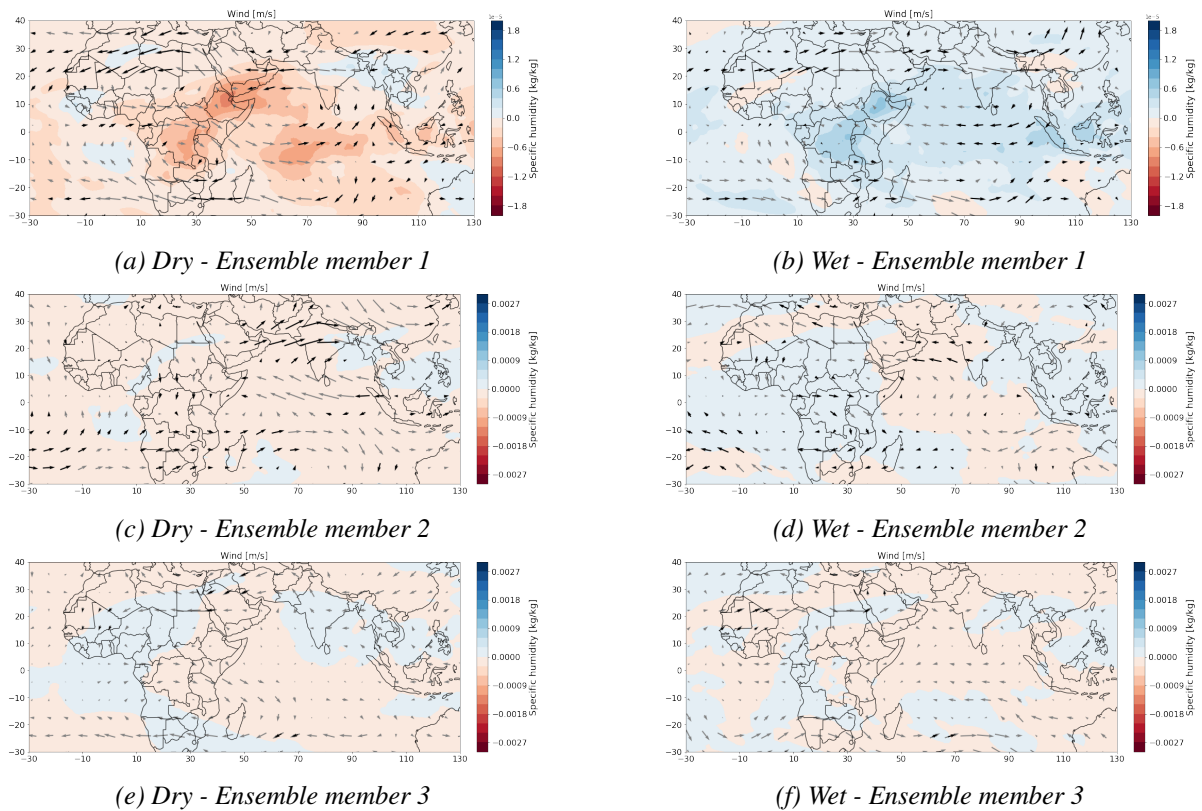


Figure 4.27: MAM wind [m/s] (200hPa) anomaly from three ensemble members of the NorESM2-MM. Dry events are shown to the left, and wet events are shown to the right. The arrows indicate the wind anomaly direction and strength. Black arrows indicate values that are significant at the 10% significance level. Grey arrows indicate non-significant values. The contour shading represents specific humidity anomalies at 200 hPa [kg/kg]. The blue shading indicates values wetter than climatology, and the red shading indicates drier than climatology.

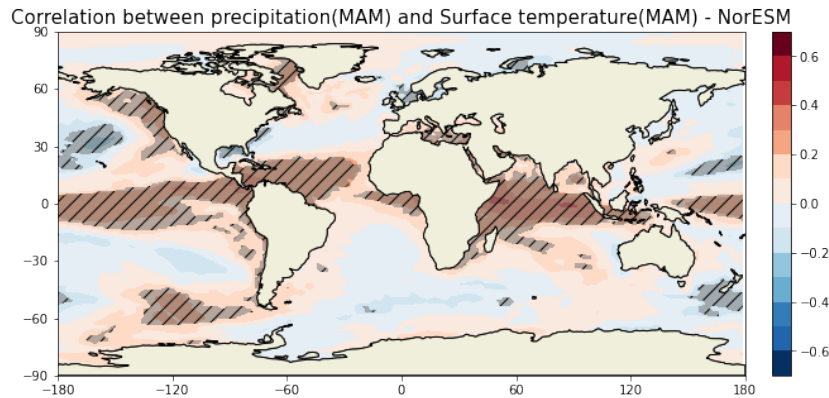


Figure 4.28: Correlation between MAM precipitation in the Belg domain and MAM surface temperature. Both variables are from the NorESM2-MM. The red color indicates a positive correlation, while the blue indicates a negative one. The shaded area corresponds to where the correlations are significant at the 10% significance level

### 4.6.3 SST - NorESM2-MM

The observations and Figure 4.8 showed that five regions stood out on the correlation plot. These were: Agulhas current, PMM-north, PMM-south, Benguela, and the Indian Ocean. Doing the same analysis to the NorESM2-MM data gives the correlation plot shown in Figure 4.28. The calculation was done by correlating surface temperature (MAM) and precipitation (MAM) in the Belg domain for each ensemble member and then taking the mean. This Figure shows a bit different result compared to the observations. The region with the highest correlation when investigating the surface temperature from the model is the Indian Ocean, which also was visible when using the observation, but with a lower correlation. Secondly, in Figure 4.28, the ENSO signal is quite visible, which was not as clear in the observations. However, a connection between La Niña and precipitation in Ethiopia was shown earlier in the analysis performed in this thesis. The results also show a small signal of the PMM patches here which also was visible when investigating the observations. The model can not capture the Agulhas or the Benguela. However, it shows a correlation between MAM precipitation in Ethiopia and the Atlantic Niño, which the observations did not capture. In conclusion, the model can capture the PMM signal and the western Indian Ocean. On the other hand, it struggles to capture the Agulhas current and the Benguela Niño.

### 4.6.4 NAO - NorESM2-MM

To continue to see if the NorESM2-MM can resemble the results from the observations, I wanted to investigate if the NAO index was visible in the model as it was in the observations. The observations (Figure 4.15) showed that a wet MAM season was associated with a positive anomaly over Iceland and a negative anomaly over the Azores (negative NAO). The effect of a positive NAO was described by previous research, but this effect is more uncertain from the analysis in this thesis. To compare this result to the model's output, I performed a composite analysis on geopotential height at 850 hPa from the NorESM2-MM model.

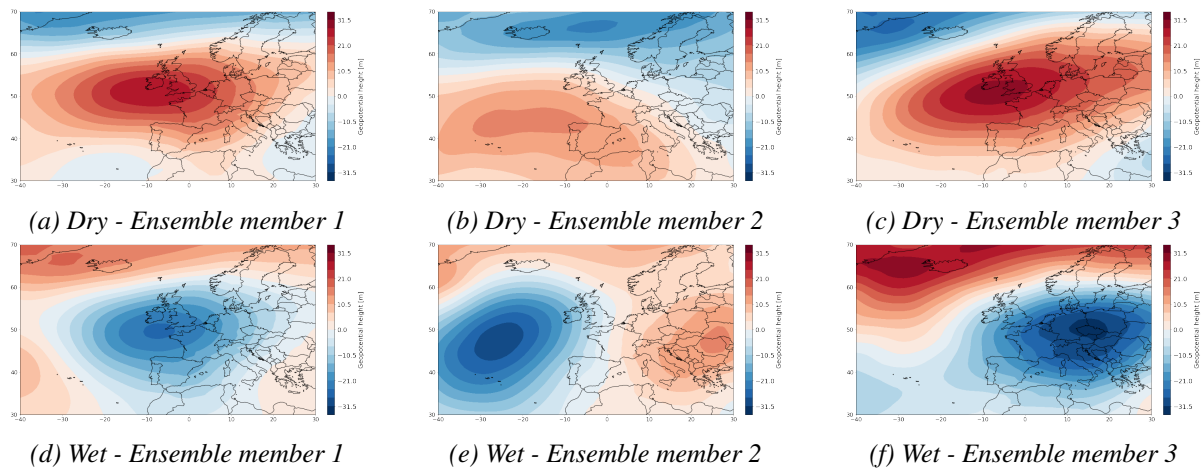


Figure 4.29: MAM geopotential height [m] (850hPa) anomaly from three ensemble members of the NorESM2-MM. Dry events are shown in the upper panel, and wet events are shown in the bottom panel. The red shading indicates a larger geopotential height than climatology, and the blue shading indicates a lower geopotential height than climatology

The geopotential height anomalies associated with dry and wet events for the three ensemble members are shown in Figure 4.29. In the dry composites in the upper panel, all ensemble members show a negative NAO index which matches the observations. However, the signal is much stronger compared to the observations. For the wet events, there is more variation between the ensemble members. A positive geopotential height anomaly is visible for the first ensemble member over Iceland. However, over the Azores, there are both positive and negative anomalies. Thereby, there might be a weakly negative NAO index in this case, but it is hard to say since the Azores don't have a clear negative signal. Ensemble members 2 and 3 show a clearer signal with a positive anomaly over Iceland and a negative anomaly over the Azores. This represents a negative NAO and, as expected, wet events. These results suggest that the NorESM2-MM can capture the NAO signal associated with dry and wet years quite well. However, this result is not significant, as expected, since the observations were not either.

## 4.7 Discussion

The result section of this thesis showed that several factors in the atmosphere and ocean affect the interannual variability of Belg rain in Ethiopia. This section will cover a discussion of these results. Does the result match the research already done on this topic? What are the limitations of this study? These are questions I will discuss in this section.

A part of the analysis in this thesis is the selection of region and timing of the Belg season. Small changes in these two factors would affect the entire analysis forward. There is some disagreement in the research in when the Belg season starts. Including February in this analysis would affect the region and further analysis. Even though the results in this thesis showed that February does not contribute as much as the other

months, including February could have some positive aspects in investigating the early stage of the Belg season. The method used in this thesis in selecting the Belg domain also differs from other studies. The studies that divided Ethiopia into several regions did this based on regions with a similar rain pattern. Due to this, there are differences in the regions used as a basis for the correlation and composite analysis, thereby the possibility of causing a difference in the results.

By linking to previous studies done on the Belg rain Nicholson (2017) discussed the contrast among the months of the Belg season. Nicholson suggests that when investigating the Belg season, the months should be treated separately due to the inhomogeneity in the factors controlling the precipitation during these months. In this thesis, I have used MAM as a whole to see which factors control precipitation during the entire period. Doing the analysis of March, April, and May separately could give another result, but time didn't permit me to check this.

When investigating the MAM precipitation in Ethiopia, I choose to use CHIRPS for precipitation due to the evaluation done on CHIRPS in Ethiopia. In addition to this, the evaluation of ERA5 showed that it struggles to represent the precipitation distribution in areas with topographic barriers. This is important in a country with such complex topography as Ethiopia has. Using ERA5 data for precipitation as a base in the composite analysis would give different wet/dry years compared to CHIRPS and also other results in the composite analysis. These years are shown in Table 4.2 and 4.1. Since I used ERA5 data for most of the variables when doing the composites, it could give a more correct result. However, to check this, I performed the composite analysis to the overlapping years marked with a star in Table 4.2 and 4.1. By investigating the wind composites for overlapping years at 850 and 200 hPa (not shown), the wind signal is weaker and more chaotic, thereby, no clear signal. However, only three years were dry in both ERA5 and CHIRPS, which might be too few to use as a base in the composites. The composites performed by using the CHIRPS year match the results from other studies to a larger degree. There are some uncertainties in the evaluation of CHIRPS over Ethiopia done by Dinku et al. (2018) due to the lack of independent stations in the southern part of Ethiopia, which is the main focus of this thesis. However, due to the good performance in the rest of Ethiopia, it is reason to believe that CHIRPS is also a good choice in the south.

Another aspect of choosing the base for the composite analysis is the number of wet and dry years. The more years to be used in the composites, the more one can trust the results. This would be possible if precipitation data from before 1981 were available. However, data before that time period would maybe not be as accurate due to the lack of satellite measurements. There are also possible to use another definition of wet and dry years that would affect the entire analysis.

The 200 hPa wind composites showed a relationship between the Subtropical Westerly

Jet and MAM precipitation in Ethiopia. This matches the results by Williams and Kniveton (2011) and Camberlin and Philippon (2002), which explains that divergence ahead of the trough induces upward motion. If this jet is shifted southward, this upward motion takes place over Ethiopia, which results in enhanced precipitation. By investigating 850 hPa wind, Williams and Kniveton (2011) also suggests that during the wet years, most of the moisture influx for the southern part of Ethiopia comes from the Atlantic Ocean due to a cyclonic anomaly over the Indian Ocean. The results from the observations show that the contribution from the Atlantic Ocean is much lower compared to the Indian Ocean. The cyclonic anomaly over the Indian Ocean is not visible in the results of this thesis. There are several reasons why these results differ from Williams and Kniveton (2011). Williams and Kniveton (2011) included February in the calculations, which was excluded in this thesis. There are also some differences in the region chosen. Even though the Belg domain used in this thesis is similar to area five in Williams and Kniveton (2011), small differences could make a difference in the composites in addition to less available data. Lastly, Williams and Kniveton (2011) used rain-gauge data for precipitation and ERA-40 re-analyses for wind compared to this thesis where CHIRPS and ERA5 were used.

In this thesis, different SST signals were investigated. The results showed a correlation between MAM precipitation in the Belg domain and five different SST signals: Agulhas current, PMM (north and south), Benguela Niño, and the Indian Ocean. The studies done on this topic have seen a connection between MAM precipitation and the Indian Ocean in addition to Benguela Niño (e.g. Jury (2015), Beyene et al. (2022)). However, these regions had the lowest correlation of the selected regions in this thesis. The regions having the most significant influence on MAM precipitation in Ethiopia from this thesis turned out to be Agulhas and the PMM signal, which has not been discussed in the previous research.

Another oceanic region that was investigated in this thesis is the ENSO signal. As mentioned earlier, there are disagreements on which degree ENSO affects Ethiopian spring rainfall. The results from this thesis suggest that a La Niña affects MAM precipitation and leads to deficit rainfall in the region. On the other hand, a connection between El Niño events and rain in the Belg domain was not visible. La Niña having an effect on MAM precipitation and El Niño doesn't might be the reason for the disagreement between the research. The same tendency takes place when investigating NAO and its effect on Ethiopian spring rainfall. The dispute in the research here might be because a negative NAO leads to excess rain, while there was no found relationship between a positive NAO index and precipitation in Ethiopia. One of the studies that saw a connection between MAM precipitation and NAO was Williams and Kniveton (2011), which explained that a negative NAO means a weaker Azores High, a southward shift in the Arabian High, which induces easterlies bringing moisture towards Ethiopia from the Indian Ocean. The relationship between a La Niña event and MAM precipitation in Ethiopia might be due to a strengthening of the walker circulation (Lau and Yang, 2003). These results showed to not be significant at the 10% significance level by performing the student's t-test on the geopotential height

and precipitation composites. It might be that there are too few observational data to identify teleconnections, especially when using composite analysis since they are based on just a few years when the precipitation anomaly is higher/lower compared to the normal state.

There seem to be several factors influencing the interannual variability of MAM rain in Ethiopia. A part of this master thesis was also to investigate if the NorESM2-MM model is able to reproduce these factors, which was found in the first part of this thesis. From this model, I had 3 ensemble members available, which were used to do the analysis. A limitation of this study is the limitation in the number of ensemble members. Using several members would decrease the uncertainty of the result. In this thesis, I used the area that stands out in the the ensemble mean MAM divided by annual mean precipitation. The result would be different if I used a different domain for each individual ensemble member. In the composite analysis, I used wet and dry years from 1981-2014. Using wet/dry years from the entire available time period (1850-2014) could give a more clear signal of the factors causing interannual variability of MAM precipitation in the model.

The results show that the model was able to capture the factors causing interannual variability in MAM precipitation in Ethiopia to a certain degree. Some of the SST signals were captured in addition to the connection with NAO. However, the model was not able to capture the 850hPa wind pattern from the composite analysis of the observations. Thereby, one way to improve the simulation of interannual variability of Belg rain is to nudge the model winds to reanalysis.

Several things differentiate this thesis from the work that's already been done on this topic. Firstly, the way of selecting the study area differs from earlier work. Earlier work has used areas with homogenous rainfall patterns, looking at entire Ethiopia or the Horn of Africa. In this thesis, the area was chosen by investigating where the monthly mean rain in MAM is larger than the climatological monthly mean. In addition to this, there were more available data at the time this thesis was written compared to some of the earlier research. This thesis also differs from other research by not only investigating the ability of NorESM2-MM to recreate the rainfall pattern in Ethiopia during MAM, but also seeing if the model is able to capture the factors driving this precipitation pattern.

# Chapter 5

## Conclusions and Future Work

This thesis aimed to investigate which parameters influence the interannual variability of Belg rain in Ethiopia. For this purpose, correlation and composite analysis were used. The results showed that Belg rain dominates in the southeastern part of Ethiopia, which is the region I used in my thesis. There is some disagreement about when the Belg season starts, but from the analysis in this thesis, it is reasonable to define the period of the Belg from March-May.

By investigating the wind at 850 hPa during MAM, the results showed that early development of the low-level Somali jet would affect the Belg rainfall in Ethiopia. Further, the composite analysis on the 850 hPa winds, showed that winds over the Indian Ocean are essential for the interannual variability of Precipitation in Ethiopia. Easterly winds over the Indian Ocean bring moist air toward Ethiopia, which can condense and become precipitation, while westerly winds bring moisture toward the eastern Indian Ocean and Ethiopia. The same analysis for 200 hPa winds showed that a southward shift in the Subtropical westerly jet might also lead to increased rainfall in Ethiopia.

By correlating MAM precipitation in the Belg domain with global SST, five areas stood out with high correlation: Agulhas current, PMM (north and south), Benguela Niño, and the Indian Ocean. Agulhas current and the PMM were the most contributing factors to MAM precipitation in Ethiopia. The connection between MAM precipitation in Ethiopia and Agulhas current is suggested to be through the Mascarene High and the Somali Jet, while the link to PMM is most likely through the Walker Circulation. These connections have not been discussed in previous research.

Further, the results showed that a negative NAO is associated with enhanced precipitation, and a La Niña event leads to deficit precipitation in Ethiopia. There was no apparent connection between positive NAO or El Niño events and MAM precipitation in Ethiopia.

The second part of this thesis was to see if the NorCPM and NorESM2-MM can capture the precipitation pattern in Ethiopia in addition to the factors found in the first part of this thesis. By investigating the NorCPM, it was clear that the model could not capture the MAM season in the southeastern part of Ethiopia. NorESM2-MM turned out to capture the Belg season in Ethiopia much better. The poor representation of the MAM precipitation in the NorCPM might be due to the topography representation used in the model. However, there are many other factors that could have caused this difference. The NorESM2-MM was used further to investigate the factors controlling the Belg season found in the first part. The model captured the NAO signal, and the SST regions stood out to a certain degree. However, the model fails to represent the wind pattern found in the observational part for both 850 hPa and 200 hPa.

The results of this thesis can contribute to improvements in seasonal forecasts of Belg rain. Many of the factors affecting the interannual variability of the Belg season found in this thesis are quite predictable and have a lagged correlation. Thereby, knowing the condition of these factors can give us information on the precipitation rate during MAM in Ethiopia. The forecasts can contribute to early warning systems so the population of Ethiopia can prepare for extreme weather conditions. This is crucial for Ethiopia because of its dependence on Agriculture.

In conclusion, the results of this thesis showed several factors affecting the interannual variability of Belg rain in Ethiopia. These factors turned out to be: Agulhas current, PMM, the subtropical westerly jet, La Niña events, and cases with negative NAO index. The predictability of these factors can be used in predicting Belg rain in Ethiopia.

For further work, it would be interesting to perform the analysis for each individual month in the Belg season, as several studies have pointed out the heterogeneity of the season. To check if the relationship between the PMM patches and the MAM precipitation is through the Walker Circulation, it could be helpful to do a composite analysis with vertical winds. Further, it would be interesting to investigate why there was a connection between MAM precipitation in Ethiopia and negative NAO and La Niña event and not for positive NAO or El Niño events. Why does this relationship only work in one way and not the other? It would also be good to use several ensemble members of the NorESM2-MM. Lastly, an exciting aspect of researching further would be to analyze the NorESM2-MM with nudging of ERA5 wind anomalies to see if this model performs better than the normal NorESM2-MM due to the poor wind representation in the NorESM2-MM.



# Appendix A

## Some appendix

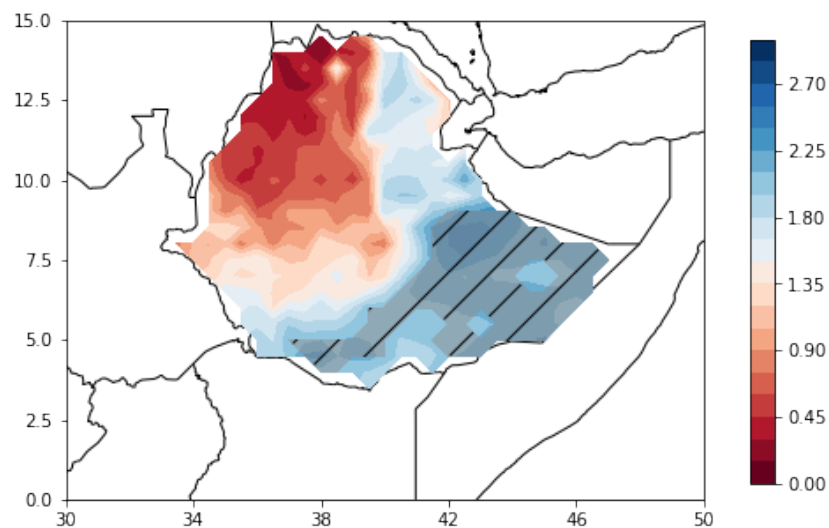


Figure A.1: The figure shows an overview of ERA5 MAM precipitation divided by annual mean over Ethiopia. The blue (red) color indicates where MAM precipitation is larger (less) than the annual mean. The shaded area represents where the values are larger than 2.

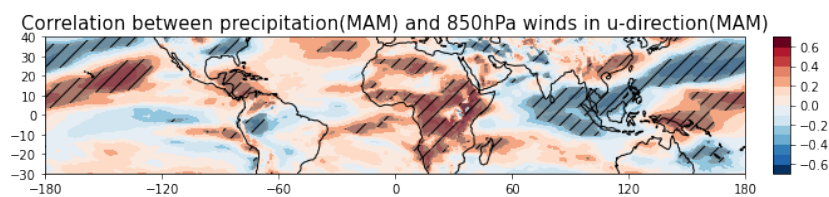


Figure A.2: Correlation between MAM precipitation in the Belg domain and MAM wind in U-direction at 850 hPa. The red color indicates a positive correlation, while the blue color indicates a negative correlation. The shaded area corresponds to where the correlations are significant at the 10% significance level.

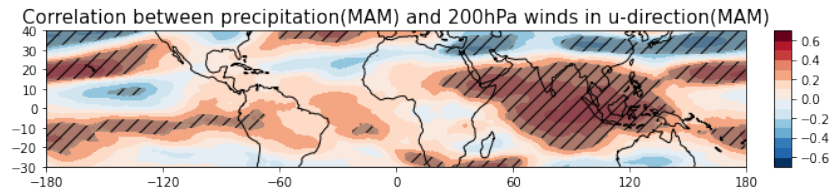


Figure A.3: Correlation between MAM precipitation in the Belg domain and MAM wind in U-direction at 200 hPa. The red color indicates a positive correlation, while the blue color indicates a negative correlation. The shaded area corresponds to where the correlations are significant at the 10% significance level.

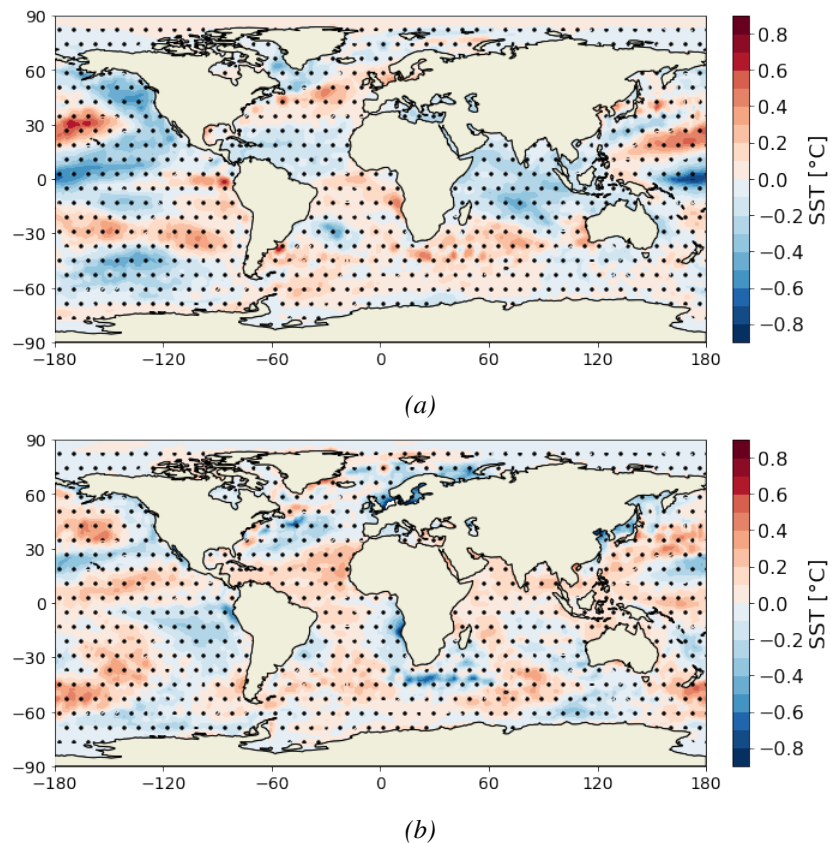


Figure A.4: SST composite from the dry and wet events in the Belg-dominated area. The values are anomalies from the climatology where red color indicates warmer than climatology and blue indicates colder. The dots indicate where the correlations are significant at the 10% significance level

# Bibliography

- Asmaa Alhamsry, Ayele Almaw Fenta, Hiroshi Yasuda, Reiji Kimura, and Katsuyuki Shimizu. Seasonal rainfall variability in ethiopia and its long-term link to global sea surface temperatures. *Water*, 12(1):55, 2019. 2.4
- Weston Anderson, Benjamin I Cook, Kim Slinski, Kevin Schwarzwald, Amy McNally, and Chris Funk. Multiyear la niña events and multiseason drought in the horn of africa. *Journal of Hydrometeorology*, 24(1):119–131, 2023. 4.3.4
- Mengesha Asefa, Min Cao, Yunyun He, Ewuketu Mekonnen, Xiaoyang Song, and Jie Yang. Ethiopian vegetation types, climate and topography. *Plant Diversity*, 42(4): 302–311, 2020. (document), 2.1, 2.1
- World Bank. Ethiopia: Accelerating equitable growth, country economic memorandum, 2007. 1
- Endalkachew Bekele-Biratu, Wassila M Thiaw, and Diriba Korecha. Sub-seasonal variability of the belg rains in ethiopia. *International Journal of Climatology*, 38 (7):2940–2953, 2018. 1, 4.1
- Ingo Bethke, Yiguo Wang, François Counillon, Noel Keenlyside, Madlen Kimmritz, Filippa Fransner, Annette Samuelsen, Helene Langehaug, Lea Svendsen, Ping-Gin Chiu, et al. Norcpm1 and its contribution to cmip6 dcpp. *Geoscientific Model Development*, 14(11):7073–7116, 2021. 3.2.2
- Tegegn Kassa Beyene, Manoj Kumar Jain, Brijesh K Yadav, and Ankit Agarwal. Multiscale investigation of precipitation extremes over ethiopia and teleconnections to large-scale climate anomalies. *Stochastic Environmental Research and Risk Assessment*, 36(5):1503–1519, 2022. 2.4, 4.7
- Jakob Bjerknes. Atmospheric teleconnections from the equatorial pacific. *Monthly weather review*, 97(3):163–172, 1969. 2.3
- Ghyslaine Boschat, Ian Simmonds, Ariaan Purich, Tim Cowan, and Alexandre Bernardes Pezza. On the use of composite analyses to form physical hypotheses: An example from heat wave–sst associations. *Scientific reports*, 6(1): 1–10, 2016. 3.3
- Elizabeth Bryan, Claudia Ringler, Barrack Okoba, Carla Roncoli, Silvia Silvestri, and Mario Herrero. Adapting agriculture to climate change in kenya: Household strategies and determinants. *Journal of environmental management*, 114:26–35, 2013. 1

- Pierre Camberlin and Nathalie Philippon. The east african march–may rainy season: Associated atmospheric dynamics and predictability over the 1968–97 period. *Journal of climate*, 15(9):1002–1019, 2002. 2.4, 4.3.2, 4.7
- Ping Chang, Li Zhang, R Saravanan, Daniel J Vimont, John CH Chiang, Link Ji, Howard Seidel, and Michael K Tippett. Pacific meridional mode and el niñosouthern oscillation. *Geophysical Research Letters*, 34(16), 2007. 2.3
- Francisco P Chavez and Monique Messié. A comparison of eastern boundary upwelling ecosystems. *Progress in Oceanography*, 83(1-4):80–96, 2009. 2.3
- Shangfeng Chen, Wenjing Shi, Zhibiao Wang, Ziniu Xiao, Wen Chen, Renguang Wu, Wanqiu Xing, and Wei Duan. Impact of interannual variation of the spring somali jet intensity on the northwest–southeast movement of the south asian high in the following summer. *Climate Dynamics*, pages 1–16, 2022. 4.3.3
- Damien Decremer, Chul E Chung, Annica ML Ekman, and Jenny Brandefelt. Which significance test performs the best in climate simulations? *Tellus A: Dynamic Meteorology and Oceanography*, 66(1):23139, 2014. 3.3
- E Di Lorenzo, G Liguori, Niklas Schneider, JC Furtado, BT Anderson, and MA Alexander. Enso and meridional modes: A null hypothesis for pacific climate variability. *Geophysical Research Letters*, 42(21):9440–9448, 2015. 2.3
- Tufa Dinku, Chris Funk, Pete Peterson, Ross Maidment, Tsegaye Tadesse, Hussein Gadain, and Pietro Ceccato. Validation of the chirps satellite rainfall estimates over eastern africa. *Quarterly Journal of the Royal Meteorological Society*, 144:292–312, 2018. 3.1, 4.2, 4.7
- Jonathan M Eden, Martin Widmann, and Gavin R Evans. Pacific sst influence on spring precipitation in addis ababa, ethiopia. *International journal of climatology*, 34(4): 1223–1235, 2014. 2.4, 4.3.1
- BD Enyew and GJ Steeneveld. Analysing the impact of topography on precipitation and flooding on the ethiopian highlands. *J. Geol. Geosci*, 3(2), 2014. 2.1
- Chris Funk, Pete Peterson, Martin Landsfeld, Diego Pedreros, James Verdin, Shraddhanand Shukla, Gregory Husak, James Rowland, Laura Harrison, Andrew Hoell, et al. The climate hazards infrared precipitation with stationsa new environmental record for monitoring extremes. *Scientific data*, 2(1):1–21, 2015. 3.1
- Chris Funk, Andreas H Fink, Laura Harrison, Zewdu Segele, Hussen Seid Endris, Gideon Galu, Diriba Korecha, and Sharon E Nicholson. Frequent but predictable droughts in east africa driven by a walker circulation intensification. *Authorea Preprints*, 2023. 1
- Mesgana Seyoum Gizaw, Getu Fana Biftu, Thian Yew Gan, Semu Ayalew Moges, and Harri Koivusalo. Potential impact of climate change on streamflow of major ethiopian rivers. *Climatic Change*, 143(3):371–383, 2017. 2.2

- Stephanie Gleixner, Noel S Keenlyside, Teferi D Demissie, François Counillon, Yiguo Wang, and Ellen Viste. Seasonal predictability of kiremt rainfall in coupled general circulation models. *Environmental Research Letters*, 12(11):114016, 2017. 1
- Stephanie Gleixner, Teferi Demissie, and Gulilat Tefera Diro. Did era5 improve temperature and precipitation reanalysis over east africa? *Atmosphere*, 11(9):996, 2020. 3.1
- David Grey and Claudia W Sadoff. Sink or swim? water security for growth and development. *Water policy*, 9(6):545–571, 2007. 1
- Sridhar Gummadi, KPC Rao, Jemal Seid, Gizachew Legesse, MDM Kadiyala, Robel Takele, Tilahun Amede, and Anthony Whitbread. Spatio-temporal variability and trends of precipitation and extreme rainfall events in ethiopia in 1980–2010. *Theoretical and Applied Climatology*, 134(3):1315–1328, 2018. 1, 2.4
- Abdel Hannachi. A primer for eof analysis of climate data. *Department of Meteorology, University of Reading*, 1:29, 2004. 3.3
- James W Hansen, Simon J Mason, Liqiang Sun, and Arame Tall. Review of seasonal climate forecasting for agriculture in sub-saharan africa. *Experimental agriculture*, 47(2):205–240, 2011. 1
- K Hansingo and CJC Reason. Modelling the atmospheric response over southern africa to sst forcing in the southeast tropical atlantic and southwest subtropical indian oceans. *International Journal of Climatology: A Journal of the Royal Meteorological Society*, 29(7):1001–1012, 2009. 2.3
- Vittal Hari, Subimal Ghosh, Wei Zhang, and Rohini Kumar. Strong influence of north pacific ocean variability on indian summer heatwaves. *Nature Communications*, 13(1):5349, 2022. 2.3, 4.3.3
- Stefan Hastenrath, Achim Nicklis, and Lawrence Greischar. Atmospheric-hydrospheric mechanisms of climate anomalies in the western equatorial indian ocean. *Journal of Geophysical Research: Oceans*, 98(C11):20219–20235, 1993. 2.4
- Tímea Haszpra, Mátyás Herein, and Tamás Bódai. Investigating enso and its teleconnections under climate change in an ensemble view—a new perspective. *Earth System Dynamics*, 11(1):267–280, 2020. 2.3
- Hans Hersbach, Bill Bell, Paul Berrisford, Shoji Hirahara, András Horányi, Joaquín Muñoz-Sabater, Julien Nicolas, Carole Peubey, Raluca Radu, Dinand Schepers, et al. The era5 global reanalysis. *Quarterly Journal of the Royal Meteorological Society*, 146(730):1999–2049, 2020. 3.1
- Andrew Hoell, Chris Funk, and Mathew Barlow. La niña diversity and northwest indian ocean rim teleconnections. *Climate dynamics*, 43(9):2707–2724, 2014. 2.4
- James W Hurrell, Yochanan Kushnir, Geir Ottersen, and Martin Visbeck. An overview of the north atlantic oscillation. *Geophysical Monograph-American Geophysical Union*, 134:1–36, 2003. 2.3

- James W Hurrell, James J Hack, Dennis Shea, Julie M Caron, and James Rosinski. A new sea surface temperature and sea ice boundary dataset for the community atmosphere model. *Journal of Climate*, 21(19):5145–5153, 2008. 3.1
- ICPAC. Immediate global action required to prevent famine in the horn of africa. *Multi-agency Drought Alert*, 2022. 1
- Mark R Jury. Climatic determinants of march may rainfall variability over southeastern ethiopia. *Climate Research*, 66(3):201–210, 2015. 2.4, 4.7
- Tae Kyun Kim. T test as a parametric statistic. *Korean journal of anesthesiology*, 68(6):540–546, 2015. 3.3
- Shunya Koseki and Rodrigue Anicet Imbol Koungue. Regional atmospheric response to the benguela niñas. *International Journal of Climatology*, 41:E1483–E1497, 2021. 2.3
- Debasis Kundu and Ayon Ganguly. *Analysis of Step-Stress Models: Existing results and some recent developments*. Academic Press, 2017. 3.3
- KM Lau and S Yang. Walker circulation. *Encyclopedia of atmospheric sciences*, 2505(2510):00450–4, 2003. 2.3, 4.7
- David A Lavers, Adrian Simmons, Freja Vamborg, and Mark J Rodwell. An evaluation of era5 precipitation for climate monitoring. *Quarterly Journal of the Royal Meteorological Society*, 2022. 3.1, 4.2
- Estifanos Lemma, Shruti Upadhyaya, and RAAJ Ramsankaran. Investigating the performance of satellite and reanalysis rainfall products at monthly timescales across different rainfall regimes of ethiopia. *International Journal of Remote Sensing*, 40(10):4019–4042, 2019. 3.1
- Arnab Maity and Michael Sherman. The two-sample t test with one variance unknown. *The American Statistician*, 60(2):163–166, 2006. 3.3
- Exavery Kisesa Makula and Botao Zhou. Coupled model intercomparison project phase 6 evaluation and projection of east african precipitation. *International Journal of Climatology*, 42(4):2398–2412, 2022. 3.2.1
- Sukeerthi Mandyam, Shanmuga Priya, Shalini Suresh, and Kavitha Srinivasan. A correlation analysis and visualization of climate change using post-disaster heterogeneous datasets. *arXiv preprint arXiv:2205.12474*, 2022. 3.3
- SA McLeod. What a p-value tells you about statistical significance. *Simply psychology*, pages 1–4, 2019. 3.3
- Gerald A Meehl. Effect of tropical topography on global climate. *Annual Review of Earth and Planetary Sciences*, 20(1):85–112, 1992. 2.1
- Ayumu Miyamoto, Hisashi Nakamura, Takafumi Miyasaka, Yu Kosaka, Bunmei Taguchi, and Kazuaki Nishii. Maintenance mechanisms of the wintertime subtropical high over the south indian ocean. *Journal of Climate*, 35(10):2989–3005, 2022. 2.3, 4.3.3

- Francis Kamau Muthoni, Vincent Omondi Odongo, Justus Ochieng, Edward M Mugalavai, Sixbert Kajumula Mourice, Irmgard Hoesche-Zeledon, Mulundu Mwila, and Mateete Bekunda. Long-term spatial-temporal trends and variability of rainfall over eastern and southern africa. *Theoretical and Applied Climatology*, 137(3): 1869–1882, 2019. 3.1
- Sharon E Nicholson. Climate and climatic variability of rainfall over eastern africa. *Reviews of Geophysics*, 55(3):590–635, 2017. 4.1, 4.7
- LJ Ogallo. Relationships between seasonal rainfall in east africa and the southern oscillation. *Journal of Climatology*, 8(1):31–43, 1988. 2.4
- John E Oliver. *Encyclopedia of world climatology*. Springer Science & Business Media, 2008. 2.2
- Philip Aming’o Omondi, Joseph L Awange, Ehsan Forootan, Laban Ayieko Ogallo, Ruben Barakiza, Gezahegn Bogale Girmaw, Isaac Fesseha, Venerabilis Kululetera, Caroline Kilembe, Mathieu Mugunga Mbat, et al. Changes in temperature and precipitation extremes over the greater horn of africa region from 1961 to 2010. *International Journal of Climatology*, 34(4):1262–1277, 2014. 1
- Vincent O Otieno and Richard O Anyah. Cmp5 simulated climate conditions of the greater horn of africa (gha). part 1: contemporary climate. *Climate dynamics*, 41(7): 2081–2097, 2013. 4.1
- Jennifer Phillips and Beverly McIntyre. Enso and interannual rainfall variability in uganda: implications for agricultural management. *International Journal of Climatology: A Journal of the Royal Meteorological Society*, 20(2):171–182, 2000. 2.4
- Parichart Promchote, S-Y Simon Wang, Yuan Shen, Paul G Johnson, and Ming-Hwi Yao. A seasonal prediction for the wet–cold spells leading to winter crop damage in northwestern taiwan with a combined empirical–dynamical approach. *International Journal of Climatology*, 38(2):571–583, 2018. 2.3
- Kavirajan Rajendran, Sajani Surendran, Stella Jes Varghese, and Anjali Sathyanath. Simulation of indian summer monsoon rainfall, interannual variability and teleconnections: evaluation of cmp6 models. *Climate Dynamics*, 58(9):2693–2723, 2022. 3.2.2
- Eugene M Rasmusson and Phillip A Arkin. A global view of large-scale precipitation variability. *Journal of Climate*, 6(8):1495–1522, 1993. 2.2
- Richard W Reynolds, Nick A Rayner, Thomas M Smith, Diane C Stokes, and Wanqiu Wang. An improved in situ and satellite sst analysis for climate. *Journal of climate*, 15(13):1609–1625, 2002. 3.1
- Eric M Roberts, NJ Stevens, Patrick M OConnor, PHGM Dirks, Michael D Gottfried, WC Clyde, RA Armstrong, AIS Kemp, and Sa Hemming. Initiation of the western branch of the east african rift coeval with the eastern branch. *Nature Geoscience*, 5 (4):289–294, 2012. 2.1

- M Rouault, Serena Illig, Ch Bartholomae, CJC Reason, and Abderrahim Bentamy. Propagation and origin of warm anomalies in the angola benguela upwelling system in 2001. *Journal of Marine Systems*, 68(3-4):473–488, 2007. 2.3
- Mathieu Rouault, Pierre Florenchie, Nicolas Fauchereau, and Chris JC Reason. South east tropical atlantic warm events and southern african rainfall. *Geophysical Research Letters*, 30(5), 2003. 2.3
- Øyvind Seland, Mats Bentsen, Dirk Olivié, Thomas Toniazzo, Ada Gjermundsen, Lise Seland Graff, Jens Bolding Debernard, Alok Kumar Gupta, Yan-Chun He, Alf Kirkevåg, et al. Overview of the norwegian earth system model (noresm2) and key climate response of cmip6 deck, historical, and scenario simulations. *Geoscientific Model Development*, 13(12):6165–6200, 2020. 3.2.1
- Jeffrey Shaman and Eli Tziperman. The effect of enso on tibetan plateau snow depth: A stationary wave teleconnection mechanism and implications for the south asian monsoons. *Journal of Climate*, 18(12):2067–2079, 2005. 2.4
- Dula Shanko and Pierre Camberlin. The effects of the southwest indian ocean tropical cyclones on ethiopian drought. *International Journal of Climatology: A Journal of the Royal Meteorological Society*, 18(12):1373–1388, 1998. 2.4
- Admasu Shiferaw et al. Productive capacity and economic growth in ethiopia. *United Nations, Department of Economics and Social Affairs*, 2017. 1
- Mxolisi E Shongwe, Geert Jan Van Oldenborgh, Bart Van den Hurk, and Maarten van Aalst. Projected changes in mean and extreme precipitation in africa under global warming. part ii: East africa. *Journal of climate*, 24(14):3718–3733, 2011. 1, 4.1
- Doug M Smith, Adam A Scaife, Rosie Eade, P Athanasiadis, Alessio Bellucci, I Bethke, R Bilbao, LF Borchert, L-P Caron, F Counillon, et al. North atlantic climate far more predictable than models imply. *Nature*, 583(7818):796–800, 2020. 2.3
- Ronald B Smith. The influence of mountains on the atmosphere. In *Advances in geophysics*, volume 21, pages 87–230. Elsevier, 1979. 3.1
- Andreas Sterl, Geert Jan van Oldenborgh, Wilco Hazeleger, and Gerrit Burgers. On the robustness of enso teleconnections. *Climate Dynamics*, 29:469–485, 2007. 2.3
- JV Sutcliffe, YP Parks, NJ Widgery, and Y Parks. The hydrology of the Nile. iahs special publication 5. *volume 12*, (5):161, 1999. 2.2
- Robel Takele, Kindie Tesfaye, and Pierre C Sibiry Traoré. Seasonal climate predictability in ethiopia: Review of best predictor sets for subseasonal to seasonal forecasting. *CCAFS Working Paper*, 2020. 1
- Guirong Tan, Brian Ayugi, Hamida Ngoma, and Victor Ongoma. Projections of future meteorological drought events under representative concentration pathways (rcps) of cmip5 over kenya, east africa. *Atmospheric research*, 246:105112, 2020. 1



- Kevin E Trenberth. The definition of el nino. *Bulletin of the American Meteorological Society*, 78(12):2771–2778, 1997. 2.3
- Kevin E Trenberth. Enso in the global climate system. *El Niño Southern Oscillation in a Changing Climate*, pages 21–37, 2020. 2.3
- Charles JR Williams and Dominic R Kniveton. *African climate and climate change: physical, social and political perspectives*, volume 43. Springer Science & Business Media, 2011. 2.4, 4.3.5, 4.7
- Tassew Woldehanna, Yisak Tafere, and Manex B Yonis. Social capital as a double-edged sword for sustained poverty escapes in ethiopia. *World Development*, 158: 105969, 2022. 1
- HJ Wright, PC Walker, and J Webster. The prediction of choice in infant feeding: a study of primiparae. *The Journal of the Royal College of General Practitioners*, 33 (253):493–497, 1983. (document), 2.2
- Shuting Yang, Yongqi Gao, Koenigk Torben, Noel Keenlyside, and François Counillon. The climate model: An arcpath tool to understand and predict climate change. In *Nordic Perspectives on the Responsible Development of the Arctic: Pathways to Action*, pages 157–180. Springer, 2021. 3.2.2
- Farhad Yazdandoost, Sogol Moradian, Ardalan Izadi, and Amir Aghakouchak. Evaluation of cmip6 precipitation simulations across different climatic zones: Uncertainty and model intercomparison. *Atmospheric Research*, 250:105369, 2021. 3.2.2
- Wei Zhang, Gabriele Villarini, and Gabriel A Vecchi. Impacts of the pacific meridional mode on rainfall over the maritime continent and australia: potential for seasonal predictions. *Climate dynamics*, 53:7185–7199, 2019. 2.3
- Zhihua Zhang and John C Moore. Chapter 6-empirical orthogonal functions. *Mathematical and physical fundamentals of climate change*, pages 161–197, 2015. 3.3
- Jens Zinke, Benjamin R Loveday, CJC Reason, W-C Dullo, and D Kroon. Madagascar corals track sea surface temperature variability in the agulhas current core region over the past 334 years. *Scientific reports*, 4(1):4393, 2014. 2.3
- Eduardo Zorita and Faustine F Tilya. Rainfall variability in northern tanzania in the march-may season (long rains) and its links to large-scale climate forcing. *Climate Research*, 20(1):31–40, 2002. 2.4